MEASUREMENTS OF FLUX DENSITIES AND GAIN CORRECTIONS AT 22460.1 MHZ ON 29-30 DECEMBER 1989

VLA TEST MEMORANDUM NO. 159

Patrick C. Crane

November 1991

The fourth run in the long-term program to monitor the flux densities of selected VLA calibrators occurred on 29-30 December 1989. (The results at 1.3cm from the second run have been reported in VLA Test Memorandum No. 149, and the weather during the third run was too bad for useful observations at 1.3cm.) The present run included 1.3cm observations in the D array of the Baars' flux-density calibrators 3C48, 3C147, 3C286, and NGC7027, plus the VLA calibrators 3C84 and 3C138. All four IFs were used - A and C centered on 22485.1 MHz and B and D, on 22435.1 MHz, with bandwidths of 50 MHz. This memorandum will describe the analysis of these observations and present the flux densities and gain-correction curves obtained.

The amplitudes measured in such interferometric observations are subject to several effects:

DELAYS: The delays on the VLA are set with a tolerance of two nanoseconds, which corresponds to a reduction in amplitude of 1.4 percent. For the point and small sources observed in this program, this effect will be constant with time for each antenna, and the amplitude effects of small delay errors will still close.

SYSTEM TEMPERATURE: The system temperatures were measured continuously using the front-end synchronous detectors on each antenna. Since the previous observations in 1985, all antennas had been equipped with cooled HEMT receivers with system temperatures of 160-170 K. Consequently, the analysis has been done for all four IFs.

ATMOSPHERIC ATTENUATION: Fortunately, the weather during the observations was good and the atmosphere was fairly dry and stable. George Martin's "TIPPER" procedure was run eight times between the beginning and end of the twenty-four-hour run. The values of zenith attenuation from antenna 23 were adopted because it had the best-determined calibration value and its results were representative of those from the other antennas. The measured values of the zenith attenuation from antenna 23 ranged between 0.063 and 0.107 (one "TIPPER" scan produced discordantly high values and was rejected.) The mean value was 0.0844 +/- 0.0026, which is almost three times greater than in 1985; the sample dispersion of 0.0137 was used to calculate the error contribution.

POINTING: The last VLA pointing run prior to our observations was on 17 December 1989. The pointing curves and residuals obtained were well behaved. The residuals were typically about 10" or 0.1 of the FWHM at 1.3cm. At this level, it was still desirable to observe in interferometer-pointing mode to measure the pointing offsets and determine corrections. The improved sensitivities of all receivers allowed us to use the standard MODCOMP integration time of 10 seconds (unlike the previous time). The standard

version of DBFILL (in ISIS) did not fill interferometer-pointing data and Gareth Hunt provided a special version to do so.

APERTURE EFFICIENCY: As the elevation of a VLA antenna changes, its surface will deform. The deformations introduce phase variations across the aperture of the antenna that cause a loss of efficiency. According to Lee King, the surfaces of the VLA antennas were set to provide maximum efficiency at an elevation of 50 degrees. Lee's model of the structure of the VLA antennas predicts the rms errors and gain corrections given in Table 1.

Table 1. Predicted Rms Surface Errors and Corrections for VLA Antennas and Average 1989 Corrections

ELEVATION (Degrees)	RMS ERROR (MM)	CORRECTION	1989 AVE
0	0.305	1.086	
10	0.254	1.059	1.091
20	0.203	1.037	1.052
30	0.140	1.018	1.021
40	0.076	1.005	1.003
50	0.000	1.000	1.000
60	0.076	1.052	1.013
70	0.152	1.021	1.042
80	0.254	1.059	1.082
90	0.330	1.102	1.130

FOCUS: The surface deformations also change the shape of the best-fit parabaloid and, consequently, the position of the focus. The corresponding focus curve has not been modeled nor measured, and the default values of the longitudinal foci were used throughout the observations.

SOURCE STRUCTURE: Except for 3C84 the sources observed are resolved at 1.3cm, even in the D array. Table 2 lists the uvlimits used in obtaining the ANTSOL solutions.

Table 2. Uvlimits Used for ANTSOL Solutions

SOURCE	UVLIMITS
3C48	0-3000nsec
3C84	None
3C138	0-2000nsec
3C147	0-2000nsec
3C286	0-8000nsec
NGC7027	0- 200nsec

NGC7027 is very heavily resolved, and the ANTSOL solutions were determined only for the thirteen antennas with baselines shorter than 200nsec (1, 6, 8, 14, 15, 16, 17, 18, 19, 20, 26, 27, and 28) and were used only to estimate pointing offsets.

ANALYSIS

The analysis of the data proceeded as follows: The special DBFILL was used to fill the interferometer-pointing data at 1.3cm into ISIS, with the submode code being used as a qualifier. The nominal pointing sequence followed in interferometer pointing is to integrate for one integration period at five positions - on, +0.5 nominal FWHM in elevation, -0.5 FWHM in elevation, +0.5 FWHM in azimuth, and -0.5 FWHM in azimuth - separated by single integration periods to move between positions, with the cycle repeating until the end of the observation. (The nominal FWHM is given by 48'/signed sum in GHz of the local oscillators for IF A or 128" in the present case.) Incomplete cycles and integrations taken while the antennas were moving were flagged. ANTSOL was run on the remaining data; the solutions were written to disk in AMP*AMP (i.e., power) format with one file for each IF. The four files were reformatted and headers were inserted - including a scan number for each pointing cycle, source name, the date and time, elevation, and zenith attenuation and uncertainty - to prepare them for input to the main analysis program. There were a total of 109 scans distributed among the six sources as listed in Table 3.

Table 3. Distribution of Scans

SOURCE	SCANS
3C48	21
3C84	20
3C138	12
3C147	20
3C286	20
NGC7027	16

The next step in the analysis was to use the pointing observations to estimate pointing offsets and beamwidths for the 26 antennas used (21 and 22 were down), four IFs per antenna, for the 93 scans (excluding NGC7027) by fitting the logs of the measured amplitudes with parabolae (i.e., fitting gaussians to the amplitudes). Measurements with discrepant offsets (larger than 0.5 of the nominal FWHM) and beamwidths (smaller than 0.5 or larger than 1.5) were identified in this process and flagged in later analysis.

This stage of the analysis provided values for several parameters listed in Table 4 - the pointing r.m.s. and FWHM were used later in the analysis and the (RCP-LCP) offset and angle are of general interest. The pointing r.m.s. measures the accuracy of a single pointing measurement and was calculated by comparing 4742 measurements of the pointing offsets in azimuth and elevation for IFs A and B or for IFs C and D. The FWHM is the average of 18294 measurements of azimuth and elevation beamwidths. The offset and angle were calculated from 4488 measurements of the differences between the pointing offsets for IFs A and C or for IFs B and D.

Table 4. Pointing and Beam Parameters

Pointing r.m.s.	2.1"
FWHM	115"
(RCP-LCP) offset	6.7"
(RCP-LCP) angle	94°

The average FWHMs in azimuth and elevation for each antenna cover the range 109-123" with the exception of the most discrepant value of 127" for the elevation FWHM for antenna 2. The average offset is 5.78 +/- 0.04 percent of the FWHM, and the average offset and angle agree well with the predicted values of six percent and 96 degrees. However, the average angles for the individual antennas range between 66 and 115 degrees with uncertainties of about 2 degrees; the most discrepant values are for antennas 3, 4, 6, 8, 17, and 19 which differ by more than 15 degrees. The sizes of the offsets range between about 5" and 9" with the extreme values occurring for antennas 3, 8, 18, 23, and 27 (low) and 12 and 24 (high).

Corrected amplitudes to be used in estimating gain corrections were calculated by applying corrections to the observed "on" amplitudes for atmospheric attenuation and for the measured pointing offsets. The uncertainties in the corrected amplitudes included contributions from the uncertainties in the atmospheric attenuation and the FWHM and in determining the pointing offsets (using the pointing r.m.s. given in Table 4 as a lower limit).

The first estimates of the gain-correction curves were obtained using the 20 scans of 3C286. The Baars' formula was used to extrapolate the flux density of 3C286 to 22460.1 MHz - 2.53 Jy. The observed gain corrections were calculated by dividing the flux density by the corrected amplitudes. The gain-correction curve for each antenna was calculated by fitting in a least-squared-error sense (and weighting according to the uncertainties described in the previous paragraph plus the uncertainty in the flux density) the observed gain corrections with Legendre polynomials of the first kind. Since theoretically the minimum of this curve is at an elevation of 50 degrees, I fit with Legendre polynomials centered on that elevation; i.e., for $x = \cos(E+40^\circ)$,

$$P_0(x) = 1,$$

$$P_1(x) = x,$$

$$P_2(x) = (3x -1)/2,$$

$$P_3(x) = x(5x -3)/2,$$

$$P_4(x) = (35x -30x +3)/8.$$

Values of n as great as 4 were required to fit the 1985 observations which included over-the-top observations. The current observations were restricted to elevations in the range 8-90 degrees and fitting with n=0-2 provided excellent fits to the data.

I then applied these first estimates of the gain-correction curves to the observations of 3C48, 3C84, 3C138, and 3C147 to obtain estimates of their flux densities at 22460.1 MHz. The procedure for calculating flux densities was for each scan to apply the appropriate gain correction to each IF, average IFs A and B together (if both are available) and IFs C and D together and apply the appropriate corrections for the measured pointing offsets, and average those two values together and apply the correction for atmospheric attenuation; the uncertainty was calculated including the uncertainties in the gain corrections, pointing offsets, FWHM, and atmospheric attenuation. The flux density for each source was calculated as the weighted average of the appropriate scan-based flux densities.

Using the Baars' flux density for 3C286 and the estimates of the flux densities of the other four sources, I used all 93 scans covering elevations between 11 and 89 degrees to obtain second estimates of the gain-correction curves. Measurements with discrepant corrections were identified at this point and flagged during subsequent analysis.

FLUX DENSITIES

After several iterations of this procedure, I obtained the final flux densities and formal errors given in Table 5 for all the sources except NGC7027. Because NGC7027 is well resolved, the original VLA data were used to determine its flux density: only data from the thirteen antennas with baselines shorter than 200 nsec (1, 6, 8, 14, 15, 16, 17, 18, 19, 20, 26, 27, 28) were used; the analysis program calculated the total corrections for atmospheric attenuation, pointing offsets, and gain variations, which were then entered manually using GTBCOR. The data were exported to AIPS and the task UVFIT was used to fit a gaussian model to the amplitudes; unfortunately, UVFIT was only able to provide a good fit when I specified the dimensions of the gaussian as the values determined for the 1985 data (6.62 +/- 0.05" x 5.51 +/- 0.06" extended at position angle -30.6 +/- 2.2 degrees). The total flux density given for NGC7027 in Table 5 is the average of the values fit separately to the RR and LL data, and the uncertainty is the formal error of that average.

Table 5. Flux Densities at 1.3cm

SOURCE	BAARS	1985	1989
3C48	1.10 0.04	1.28 0.01	1.24 0.02
3C84		41.32 0.25	36.77 0.35
3C138		1.17 0.01	1.14 0.02
3C147	1.68 0.06	1.83 0.01	1.80 0.02
3C286	2.53 0.09	2.52 0.01	2.52 0.03
NGC7027	5.85 0.56	5.67 0.02	5.58 0.02

The formal errors are larger for the 1989 measurements than for the 1985 measurements, largely because of the greater value for (and uncertainty in) the atmospheric attenuation. 3C84 is the only source to show a significant change in flux density (10.5 sigma) although 3C48, 3C138, and 3C147 all decreased by about one sigma. Because of the complex procedure followed to determine the flux densities of NGC7027 for the two epochs, the actual uncertainties must be larger than those listed, but the close agreement shows that 3C286 - used as the reference - has not varied significantly between the two epochs.

GAIN CURVES

The gain-correction curves and the observed data are shown in Figures 1-26 for the 26 antennas used (excluding 21 and 22) with each IF shown separately. The uncertainties in the observed corrections are indicated by the error bars associated with the individual data points. The gain-correction curves +/- one sigma are also shown. All antennas show good

agreement between the four IFs. The coefficients of the gain-correction curves and their uncertainties are given in Table 6 normalized to unity correction at an elevation of 50 degrees and averaged over the four IFs. The gain-correction curves are well determined for the elevation range 8-90 degrees with uncertainties of about one percent using only second-order polynomials; the higher-order polynomials needed to fit the over-the-top observations in 1985 are not required.

The 26 gain-correction curves are superimposed in Figure 27. Most of the curves are close to the theoretical curve tabulated in Table 1; the last column in the Table 1 lists the corrections averaged over all 26 antennas. The average gain correction is about three percent higher than the theoretical values at 10 and 90 degrees. The antennas with the most discrepant gain-correction curves are 1, 2, 5, 18, 19, and 27. The range of variation among the curves is much less than shown in the similar plot (Memo No. 149, Figure 2) for the 1985 observations even over the range 8-90 degrees elevation. The current observations are more sensitive, better sampled (93 instead of 51 scans), and do not include over-the-top observations. The four IFs provide a consistency check and have been averaged in Table 6. The remaining variations may be explained by offsets in the longitudinal foci.

DISCUSSION

The gain-correction curves determined from the 1989 observations are much better than those from the 1985 observations - with uncertainties in the coefficients a factor of ten smaller because of better sensitivity, more samples, and the lack of over-the-top observations. Only second-order polynomials were required to fit the curves in the absence of over-the-top observations. The uncertainties in the gain curves are about one percent.

On the other hand, despite the improved gain curves, the uncertainties in the flux densities are greater for the 1989 observations. As I said above, the formal uncertainties in the flux densities are dominated by the larger value of, and the uncertainty in, the atmospheric attenuation. Only 3C84 has varied significantly between the two epochs, by about 4.5 Jy.

The gain-correction curves have been implemented in a Fortran program on ZIA called KCOR89; an example of how to run this program is given in the Appendix. For each elevation specified KCOR89 lists the gain corrections for all antennas except 21 and 22 (nominally 1) and the average correction for the 26 antennas, the corresponding voltage corrections for GTBCOR or CLCOR, and the average voltage correction if an array-averaged value is desired. Unfortunately, the corrections must still be applied manually.

The present observations allow us to examine several characteristics of the VLA antennas for discrepant behavior. These results are summarized in Table 7.

Table 7. Discrepant Antennas

FWHM	2
(RCP-LCP) offset	3, 8, 12, 18, 23, 24, 27
(RCP-LCP) angle	3, 4, 6, 8, 17, 19
Gain-correction curve	1, 2, 5, 18, 19, 27

Table 6. Coefficients of Antenna Gain-Correction Curves

ANTENNA	C0	C1	C2
1 AVERAGE	0.11217E+01	0.42371E+00	0.24332E+00
	0.10322E-01	0.14559E-01	0.22368E-01
2 AVERAGE	0.10695E+01	0.24267E+00	0.13901E+00
	0.78319E-02	0.11097E-01	0.17920E-01
3 AVERAGE	0.10960E+01	-0.90915E-01	0.19207E+00
	0.57138E-02	0.76810E-02	0.13725E-01
4 AVERAGE	0.10916E+01	-0.21435E-01	0.18318E+00
	0.71285E-02	0.96171E-02	0.16894E-01
5 AVERAGE	0.10709E+01	-0.16317E+00	0.14184E+00
	0.70302E-02	0.93130E-02	0.17145E-01
6 AVERAGE	0.10601E+01	-0.34133E-01	0.12016E+00
	0.52141E-02	0.70809E-02	0.12491E-01
7 AVERAGE	0.11034E+01	-0.14479E+00	0.20680E+00
	0.76594E-02	0.10099E-01	0.18641E-01
8 AVERAGE	0.10865E+01	-0.10017E+00	0.17296E+00
	0.68495E-02	0.91470E-02	0.16546E-01
9 AVERAGE	0.10625E+01	-0.73468E-01	0.12499E+00
	0.58012E-02	0.76292E-02	0.14095E-01
10 AVERAGE	0.10671E+01	-0.68493E-01	0.13424E+00
	0.66190E-02	0.88626E-02	0.15989E-01
11 AVERAGE	0.10784E+01	0.69334E-01	0.15689E+00
	0.62967E-02	0.86406E-02	0.14791E-01
12 AVERAGE	0.11144E+01	-0.11591E+00	0.22884E+00
	0.53852E-02	0.71636E-02	0.12988E-01
13 AVERAGE	0.10524E+01	0.70823E-01	0.10471E+00
	0.54936E-02	0.75581E-02	0.13038E-01
14 AVERAGE	0.10699E+01	-0.62437E-01	0.13987E+00
	0.49339E-02	0.66155E-02	0.11843E-01
15 AVERAGE	0.10604E+01	-0.78091E-01	0.12086E+00
	0.70578E-02	0.96074E-02	0.17022E-01
16 AVERAGE	0.10960E+01	0.37381E-01	0.19206E+00
	0.61310E-02	0.84346E-02	0.14031E-01
17 AVERAGE	0.11206E+01	-0.34977E-02	0.24121E+00
	0.60433E-02	0.80803E-02	0.14436E-01
18 AVERAGE	0.10947E+01	0.15272E+00	0.18934E+00
	0.62030E-02	0.86448E-02	0.14299E-01
19 AVERAGE	0.11162E+01	-0.17789E+00	0.23238E+00
	0.63506E-02	0.83186E-02	0.15236E-01
20 AVERAGE	0.11466E+01	-0.32831E-01	0.29320E+00
	0.96047E-02	0.13683E-01	0.19765E-01
23 AVERAGE	0.10963E+01	-0.62775E-01	0.19252E+00
	0.76275E-02	0.10378E-01	0.18367E-01
24 AVERAGE	0.10575E+01	-0.30810E-01	0.11498E+00
	0.47778E-02	0.64809E-02	0.11467E-01
25 AVERAGE	0.10779E+01	-0.14260E+00	0.15578E+00
	0.56256E-02	0.73071E-02	0.13625E-01
26 AVERAGE	0.10885E+01	0.10828E-01	0.17697E+00
	0.67017E-02	0.92094E-02	0.15383E-01
27 AVERAGE	0.11471E+01	-0.34943E+00	0.29428E+00
	0.65042E-02	0.83725E-02	0.15975E-01
28 AVERAGE	0.10695E+01	-0.29862E-01	0.13898E+00
	0.70377E-02	0.97170E-02	0.15964E-01
ALL-ANTENNA	0.10891E+01	-0.29817E-01	0.17813E+00
AVERAGE	0.13204E-02	0.17979E-02	0.30870E-02

Fourteen different antennas appear in Table 7 - 1, 2, 3, 4, 5, 6, 8, 12, 17, 18, 19, 23, 24, and 27; 2, 3, 8, 18, 19, and 27 each appear twice. Antennas 1, 23, and 27 appear on C. Wade's list of six antennas with high pointing residuals; the other three are 7, 21 (not available), and 25. Antennas 1, 4, 17, 18, 19, and 23 are among those with suspected azimuth bearing problems; the other three are 16, 21 (not available), and 28.

The origins of the discrepant (RCP-LCP) offsets and angles are unclear. There is no obvious relation between discrepant offsets and angles and the FWHMs or gain-correction curves or even between a discrepant offset and a discrepant angle (only antennas 3 and 8 have both). The offset is a differential measure that is more sensitive to minor asymmetries in the beam shapes than the global measures such as the FWHM and gain-correction curve and is more sensitive to noise (based upon the pointing r.m.s. in Table 4, any individual measurement of an offset is only two sigma.)

APPENDIX Sample Execution of the Program KCOR89

```
zia% /u/pcrane/kcor89
TYPE IN NUMBER (<=20) OF ELEVATIONS DESIRED
1
TYPE IN VALUES OF ELEVATIONS DESIRED
25
1.3CM GAIN CORRECTIONS AND ERRORS AT  25.00 DEGREES ELEVATION BASED UPON
OBSERVATIONS OF 89DEC29-30

  1    1.2443    0.0131
  2    1.1398    0.0100
  3    1.0130    0.0073
  4    1.0400    0.0091
  5    0.9690    0.0090
  6    1.0178    0.0067
  7    0.9942    0.0098
  8    1.0040    0.0088
  9    1.0024    0.0074
 10    1.0070    0.0085
 11    1.0713    0.0080
 12    1.0123    0.0069
 13    1.0580    0.0070
 14    1.0111    0.0063
 15    0.9993    0.0091
 16    1.0672    0.0078
 17    1.0631    0.0077
 18    1.1153    0.0079
 19    0.9871    0.0081
 20    1.0647    0.0121
 21    1.0000    0.0000
 22    1.0000    0.0000
 23    1.0251    0.0098
 24    1.0178    0.0061
 25    0.9815    0.0072
 26    1.0520    0.0085
 27    0.9311    0.0083
 28    1.0246    0.0090
AVE    1.0352    0.0017
VOLTAGE CORRECTIONS TO ENTER IN GTBCOR OR CLCOR

 1    1.1155
 2    1.0676
 3    1.0065
 4    1.0198
 5    0.9844
 6    1.0089
 7    0.9971
 8    1.0020
 9    1.0012
10    1.0035
11    1.0350
12    1.0061
13    1.0286
14    1.0055
15    0.9997
16    1.0331
17    1.0311
18    1.0561
19    0.9935
20    1.0318
21    1.0000
22    1.0000
23    1.0125
24    1.0089
25    0.9907
26    1.0257
27    0.9649
28    1.0122
AVERAGE VOLTAGE CORRECTION TO ENTER IN GTBCOR OR CLCOR  1.0170
```

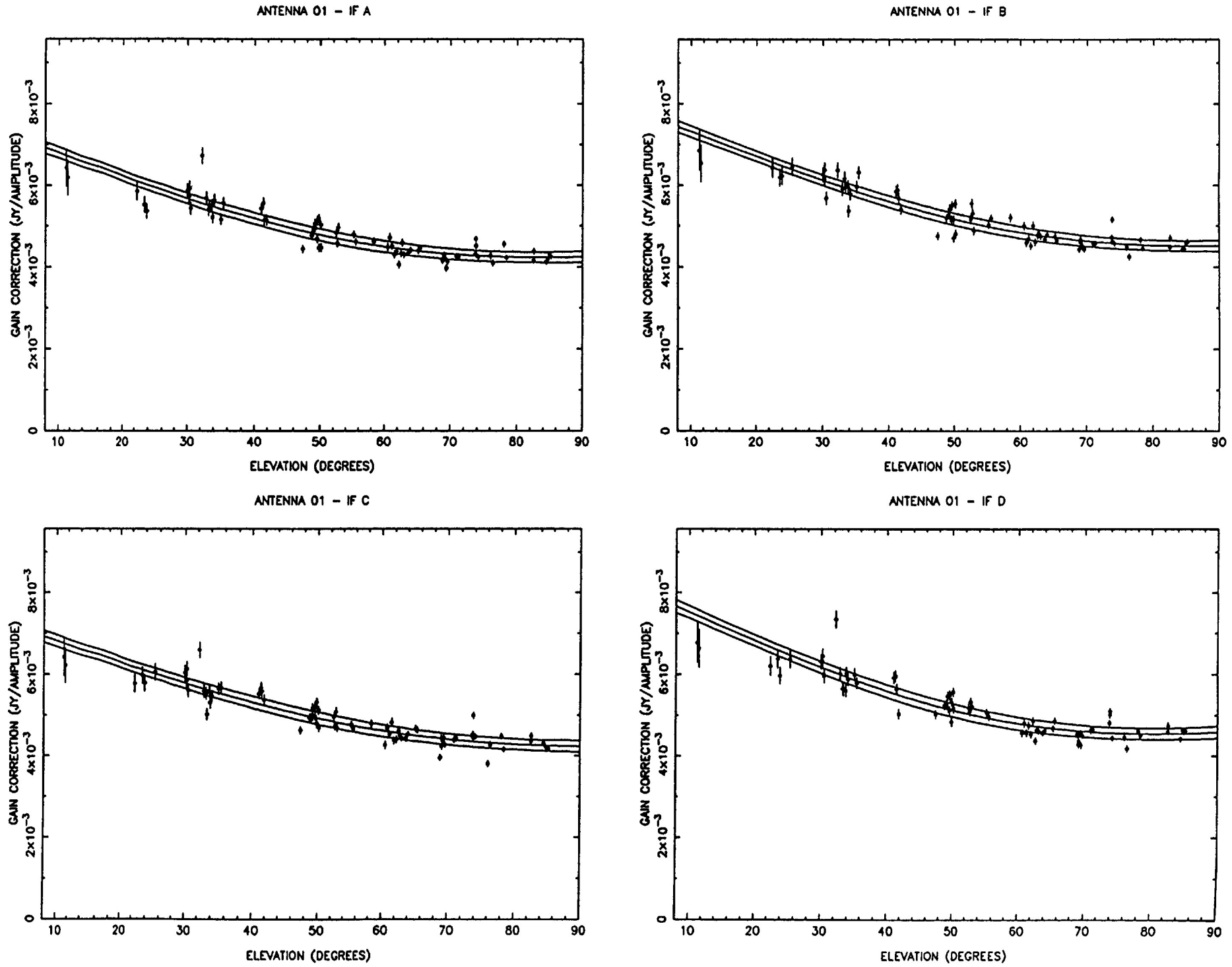
ANTENNA 01 - IF A
ANTENNA 01 - IF B
ANTENNA 01 - IF C
ANTENNA 01 - IF D
GAIN CORRECTION (JY/AMPLITUDE)
0
2x10^-3
4x10^-3
6x10^-3
8x10^-3
10
20
30
40
50
60
70
80
90
ELEVATION (DEGREES)

FIGURE 1

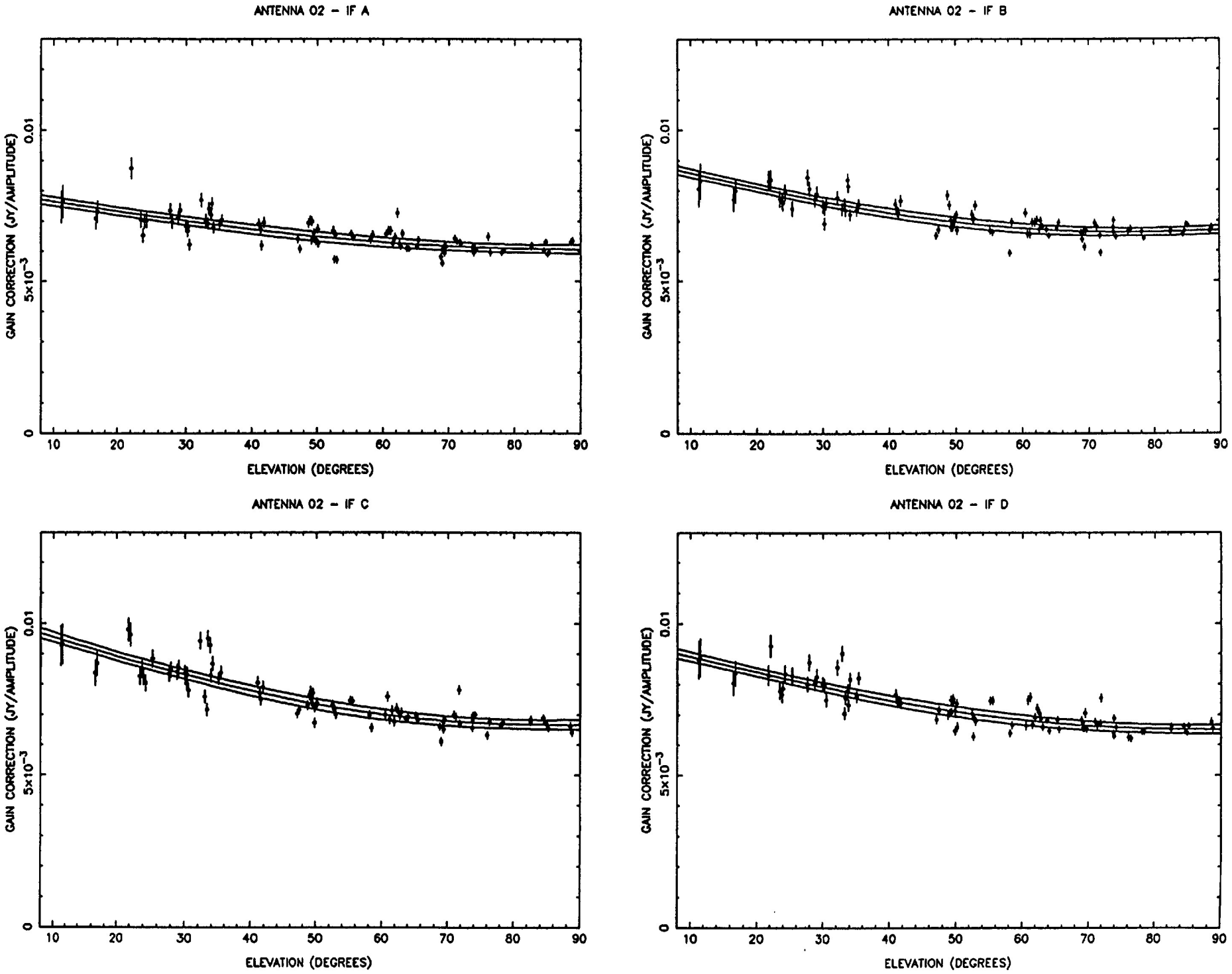
ANTENNA 02 - IF A
ANTENNA 02 - IF B
ANTENNA 02 - IF C
ANTENNA 02 - IF D
GAIN CORRECTION (JY/AMPLITUDE)
0
5x10^-3
0.01
10
20
30
40
50
60
70
80
90
ELEVATION (DEGREES)

FIGURE 2

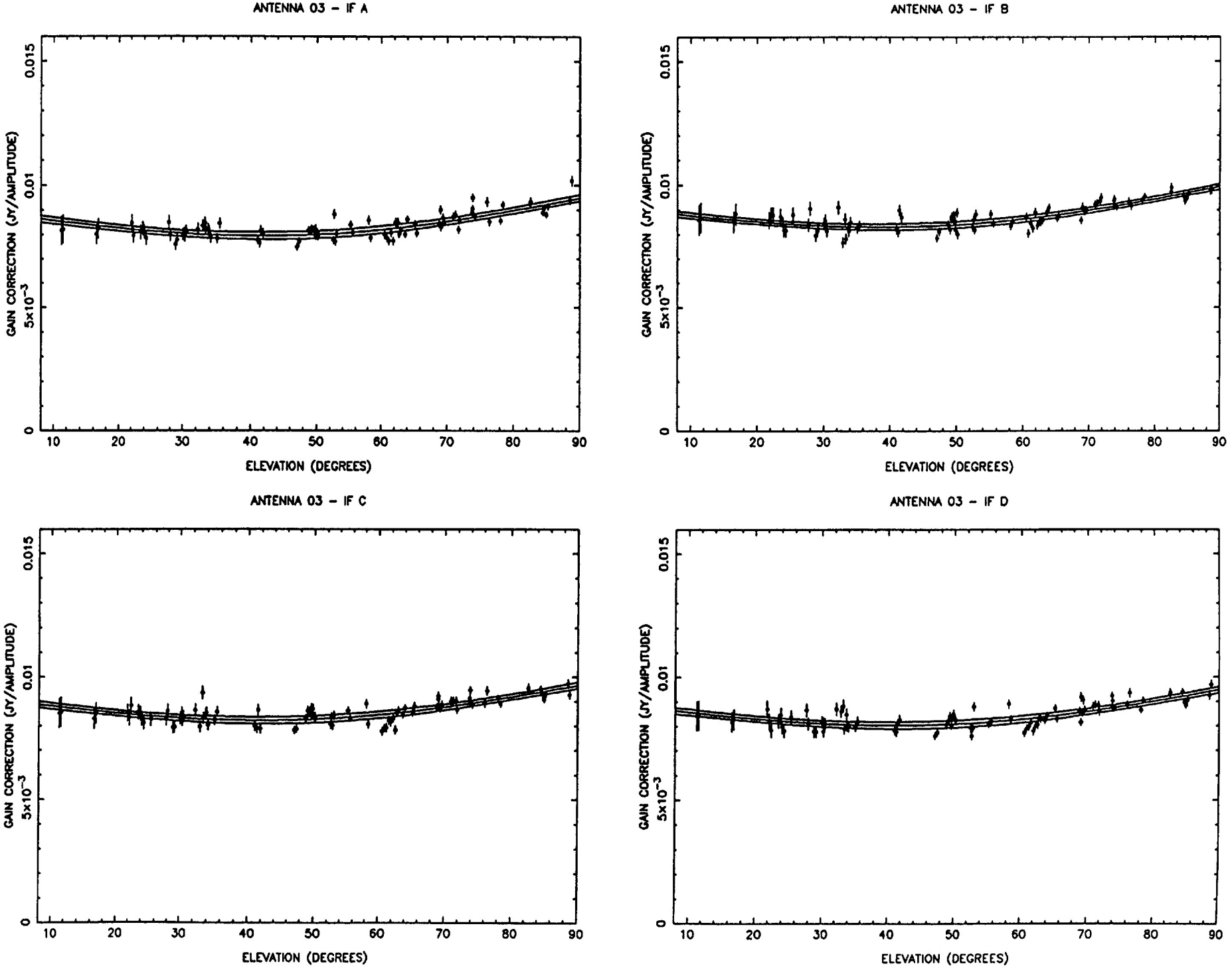
ANTENNA 03 - IF A
ANTENNA 03 - IF B
ANTENNA 03 - IF C
ANTENNA 03 - IF D
GAIN CORRECTION (JY/AMPLITUDE)
0
5x10^-3
0.01
0.015
10
20
30
40
50
60
70
80
90
ELEVATION (DEGREES)

FIGURE 3

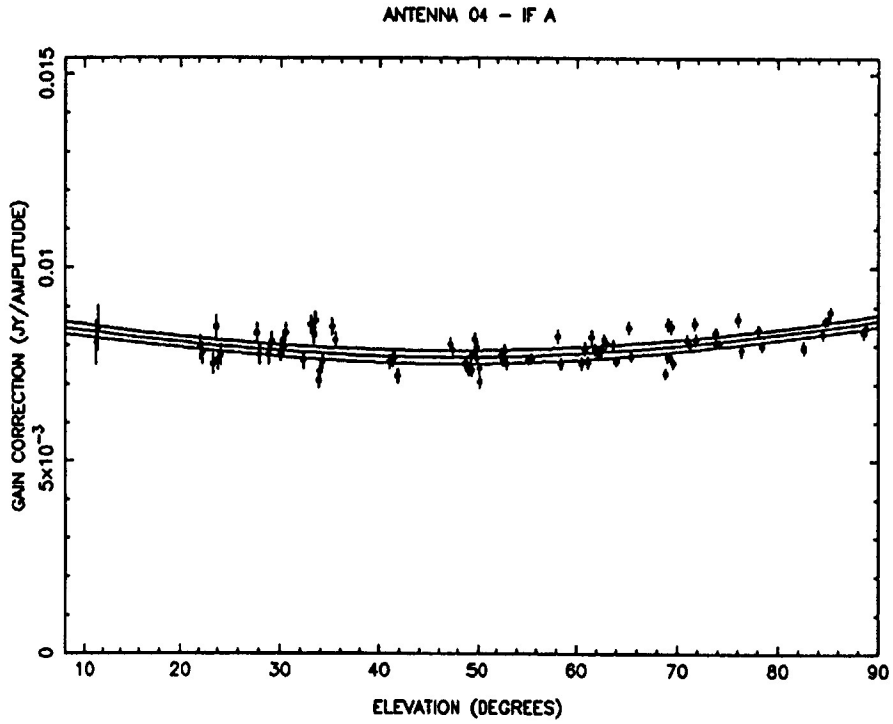
ANTENNA 04 - IF A
GAIN CORRECTION (JY/AMPLITUDE)
0
5x10⁻³
0.01
0.015
10
20
30
40
50
60
70
80
90
ELEVATION (DEGREES)

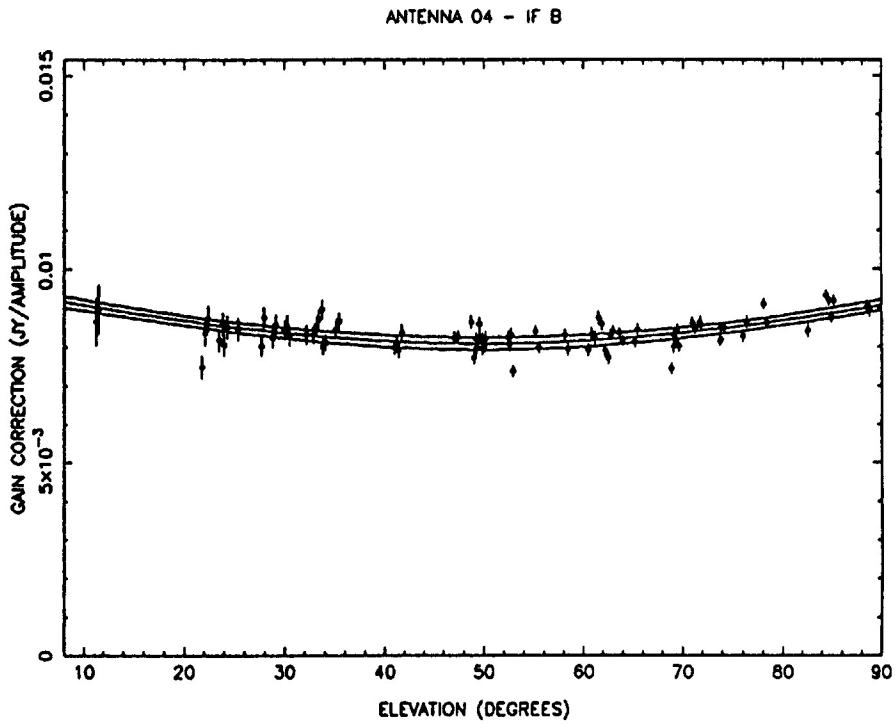
ANTENNA 04 - IF B
GAIN CORRECTION (JY/AMPLITUDE)
0
5x10⁻³
0.01
0.015
10
20
30
40
50
60
70
80
90
ELEVATION (DEGREES)

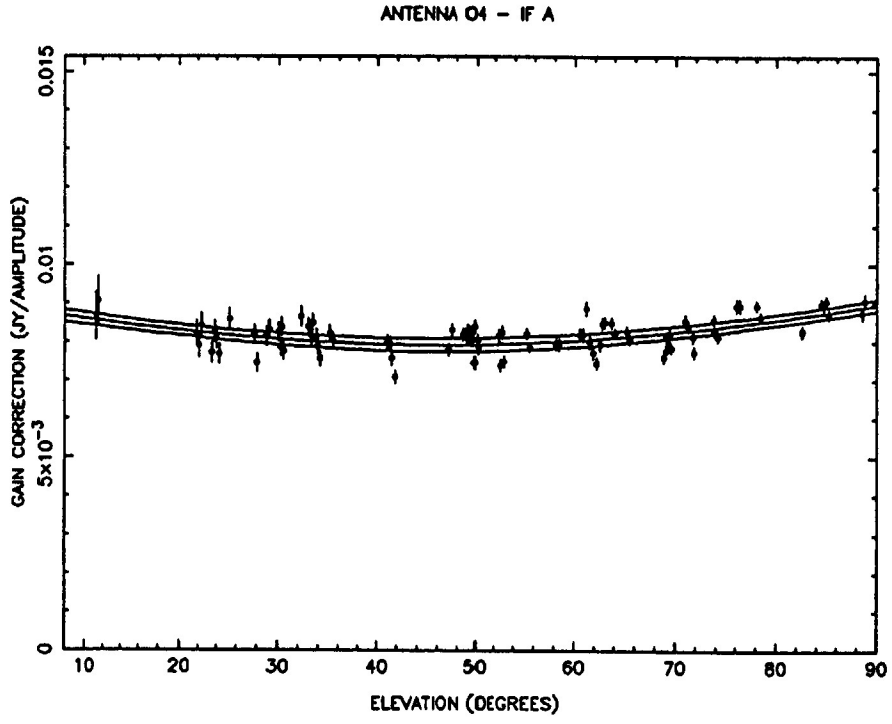
ANTENNA 04 - IF A
GAIN CORRECTION (JY/AMPLITUDE)
0
5x10⁻³
0.01
0.015
10
20
30
40
50
60
70
80
90
ELEVATION (DEGREES)

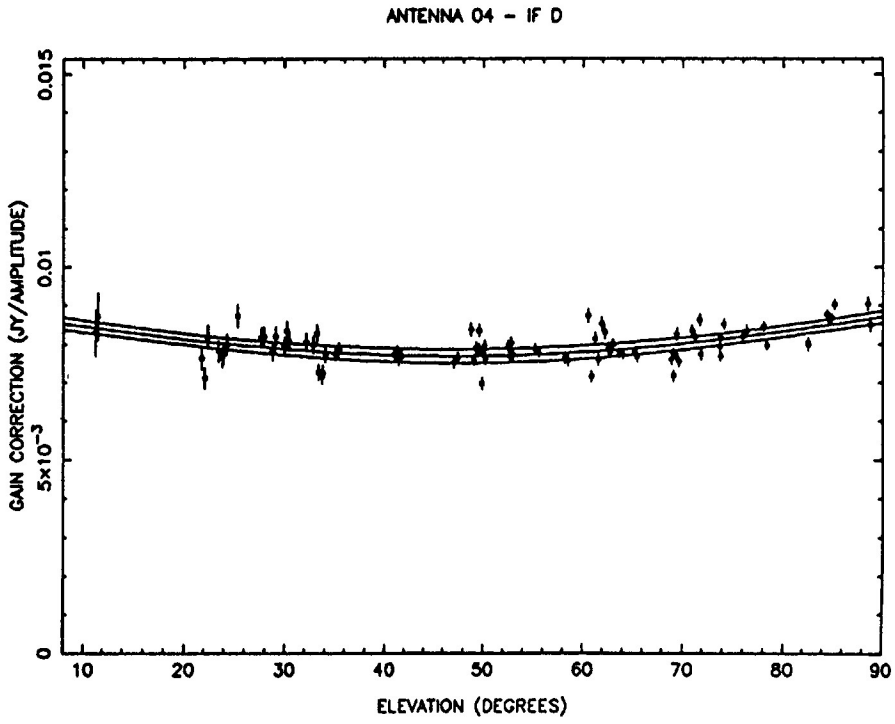
ANTENNA 04 - IF D
GAIN CORRECTION (JY/AMPLITUDE)
0
5x10⁻³
0.01
0.015
10
20
30
40
50
60
70
80
90
ELEVATION (DEGREES)

FIGURE 4

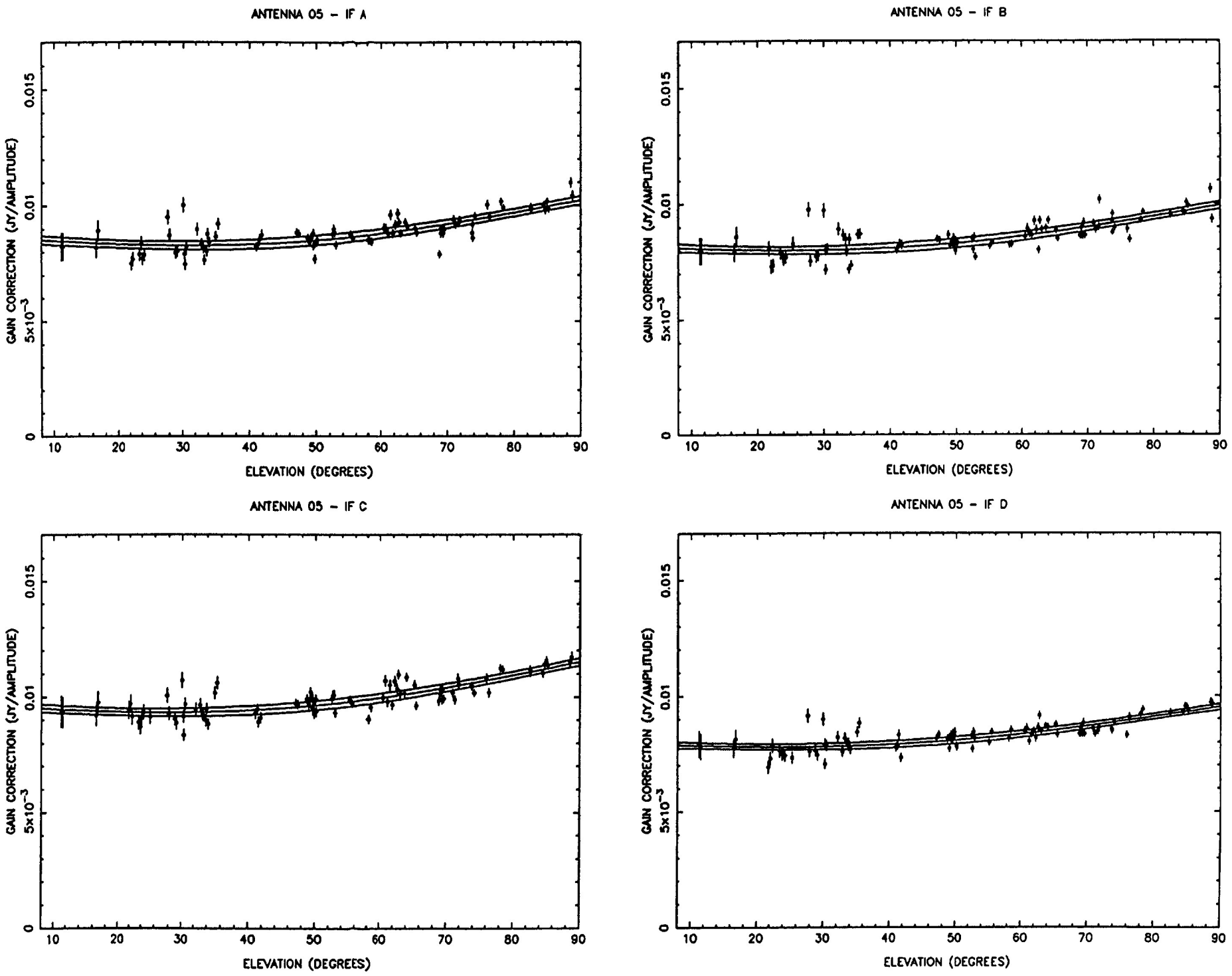
ANTENNA 05 - IF A
ANTENNA 05 - IF B
ANTENNA 05 - IF C
ANTENNA 05 - IF D
GAIN CORRECTION (JY/AMPLITUDE)
0
5x10⁻³
0.01
0.015
10
20
30
40
50
60
70
80
90
ELEVATION (DEGREES)

FIGURE 5

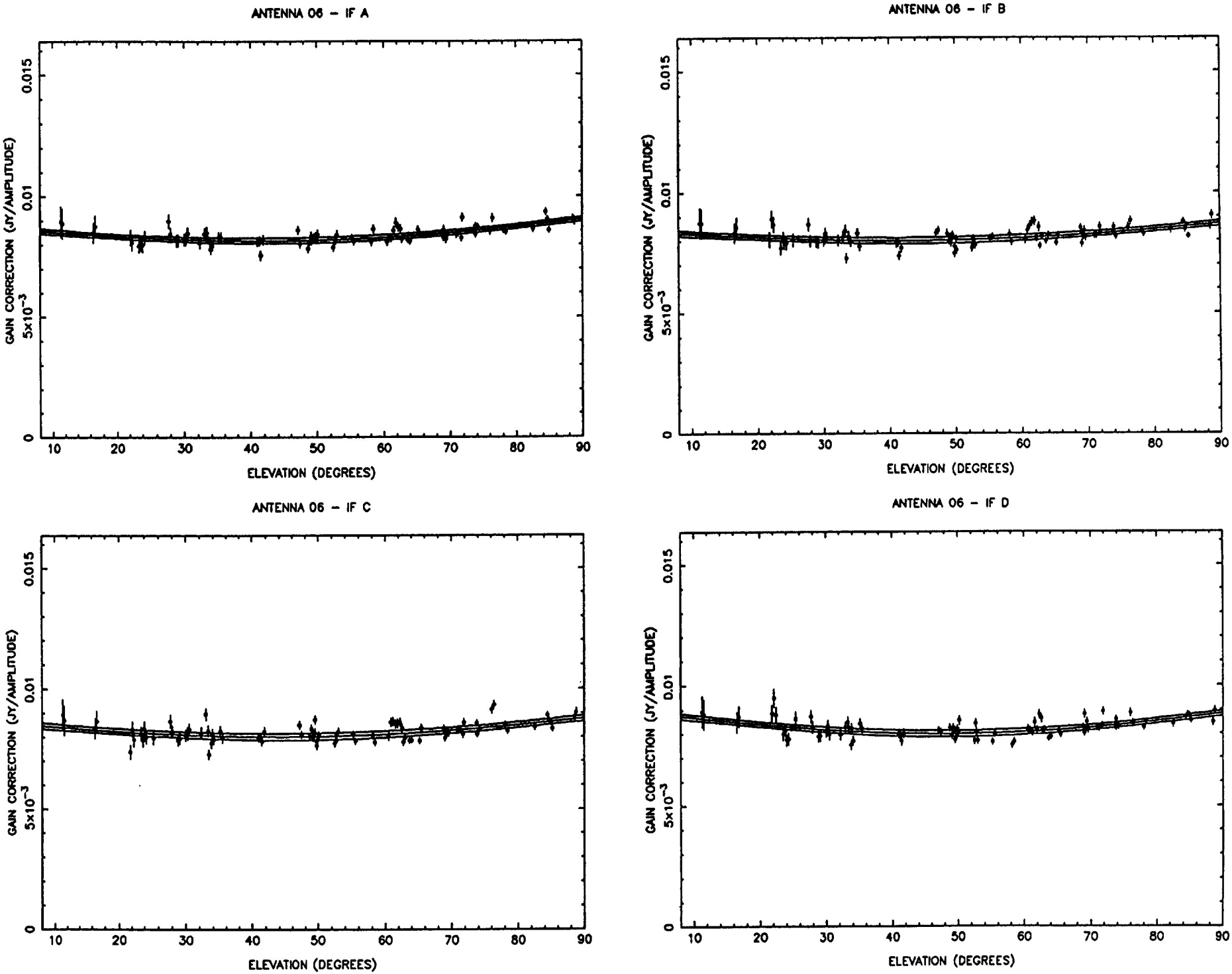
ANTENNA 06 - IF A
ANTENNA 06 - IF B
ANTENNA 06 - IF C
ANTENNA 06 - IF D
GAIN CORRECTION (JY/AMPLITUDE)
0
5x10⁻³
0.01
0.015
10
20
30
40
50
60
70
80
90
ELEVATION (DEGREES)

FIGURE 6

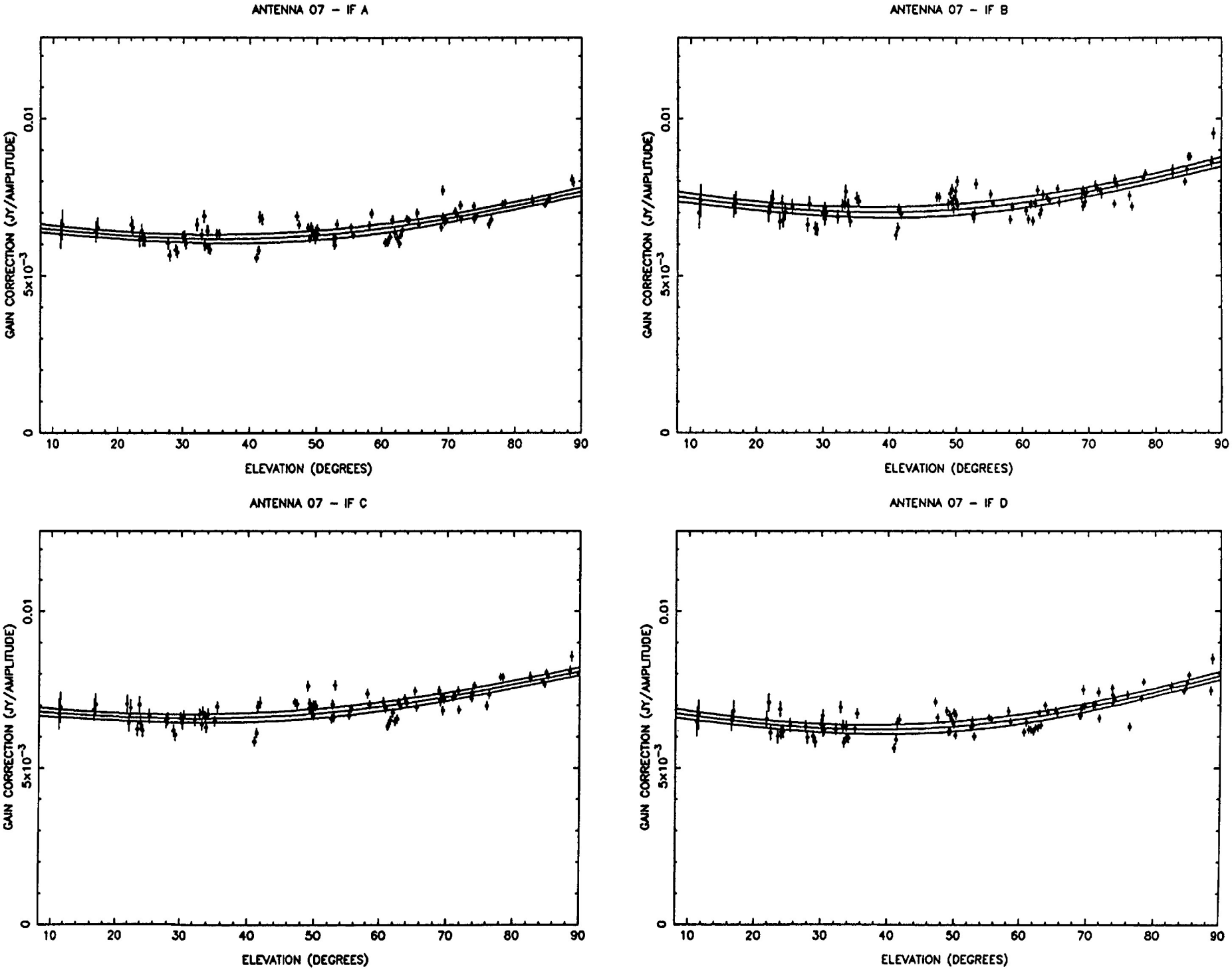
ANTENNA 07 - IF A
ANTENNA 07 - IF B
ANTENNA 07 - IF C
ANTENNA 07 - IF D
GAIN CORRECTION (JY/AMPLITUDE)
0
5x10^-3
0.01
10
20
30
40
50
60
70
80
90
ELEVATION (DEGREES)

FIGURE 7

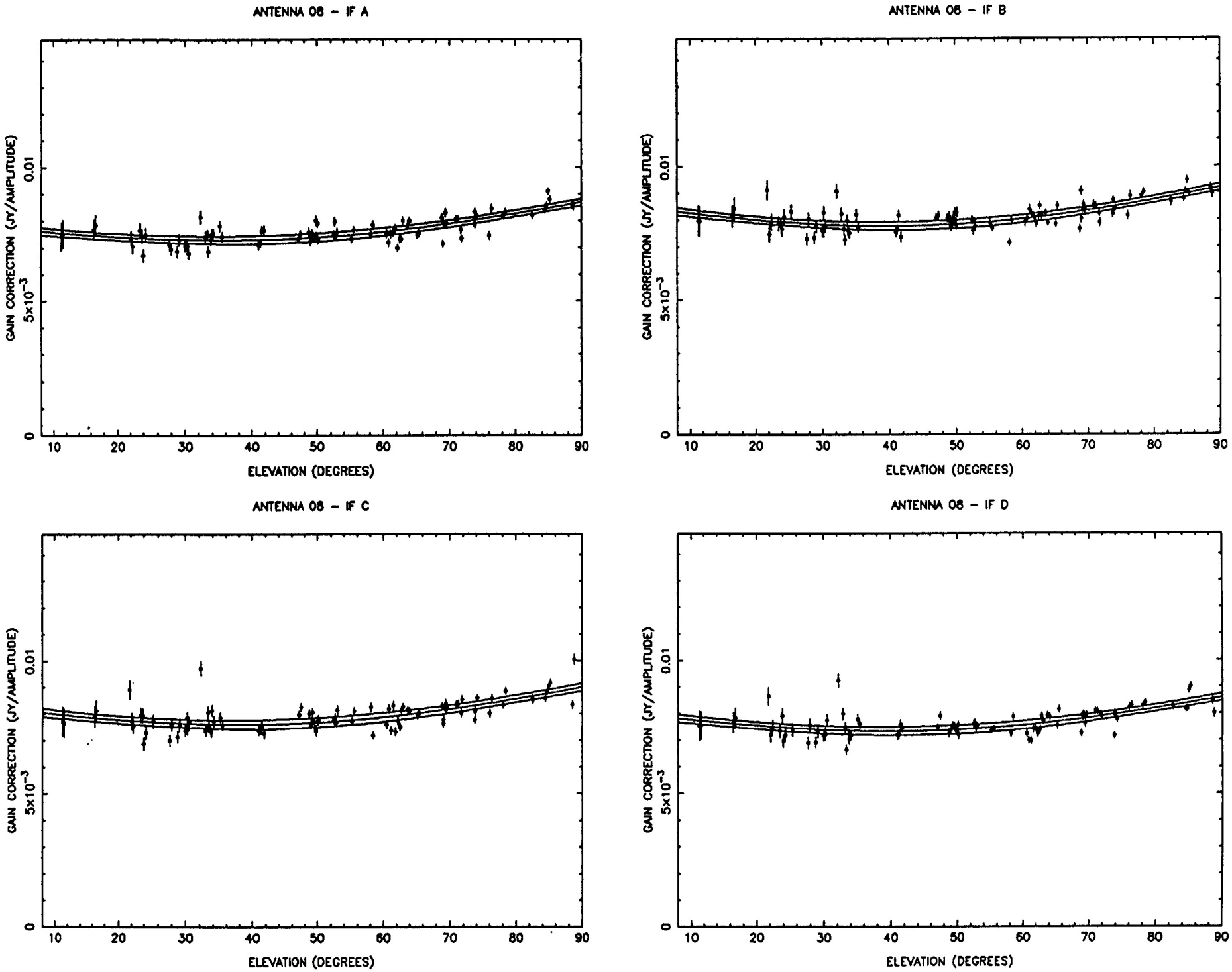
ANTENNA 08 - IF A
ANTENNA 08 - IF B
ANTENNA 08 - IF C
ANTENNA 08 - IF D
GAIN CORRECTION (JY/AMPLITUDE)
0
5x10^-3
0.01
10
20
30
40
50
60
70
80
90
ELEVATION (DEGREES)

FIGURE 8

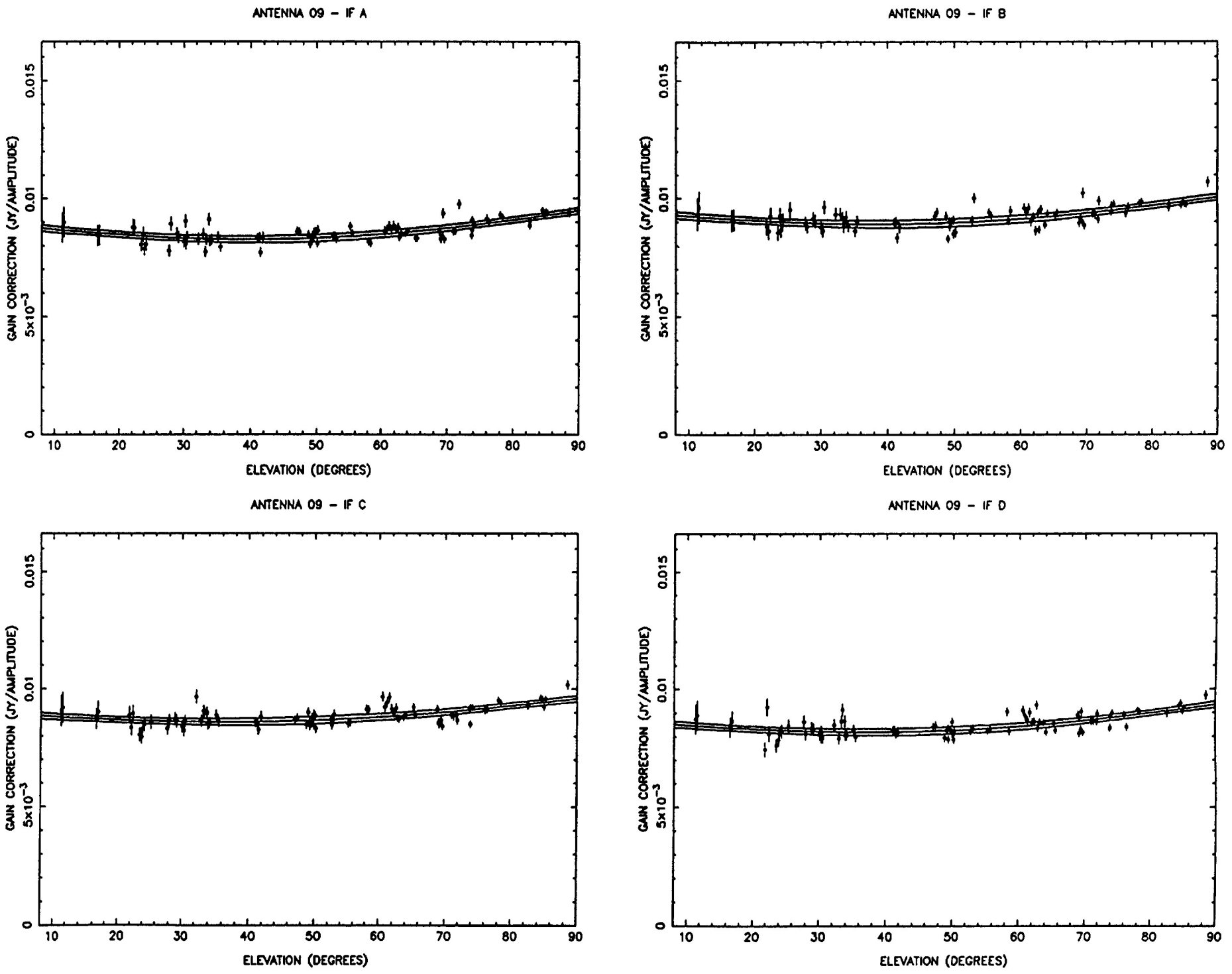
ANTENNA 09 - IF A
ANTENNA 09 - IF B
ANTENNA 09 - IF C
ANTENNA 09 - IF D
GAIN CORRECTION (JY/AMPLITUDE)
0
5x10⁻³
0.01
0.015
10
20
30
40
50
60
70
80
90
ELEVATION (DEGREES)

FIGURE 9

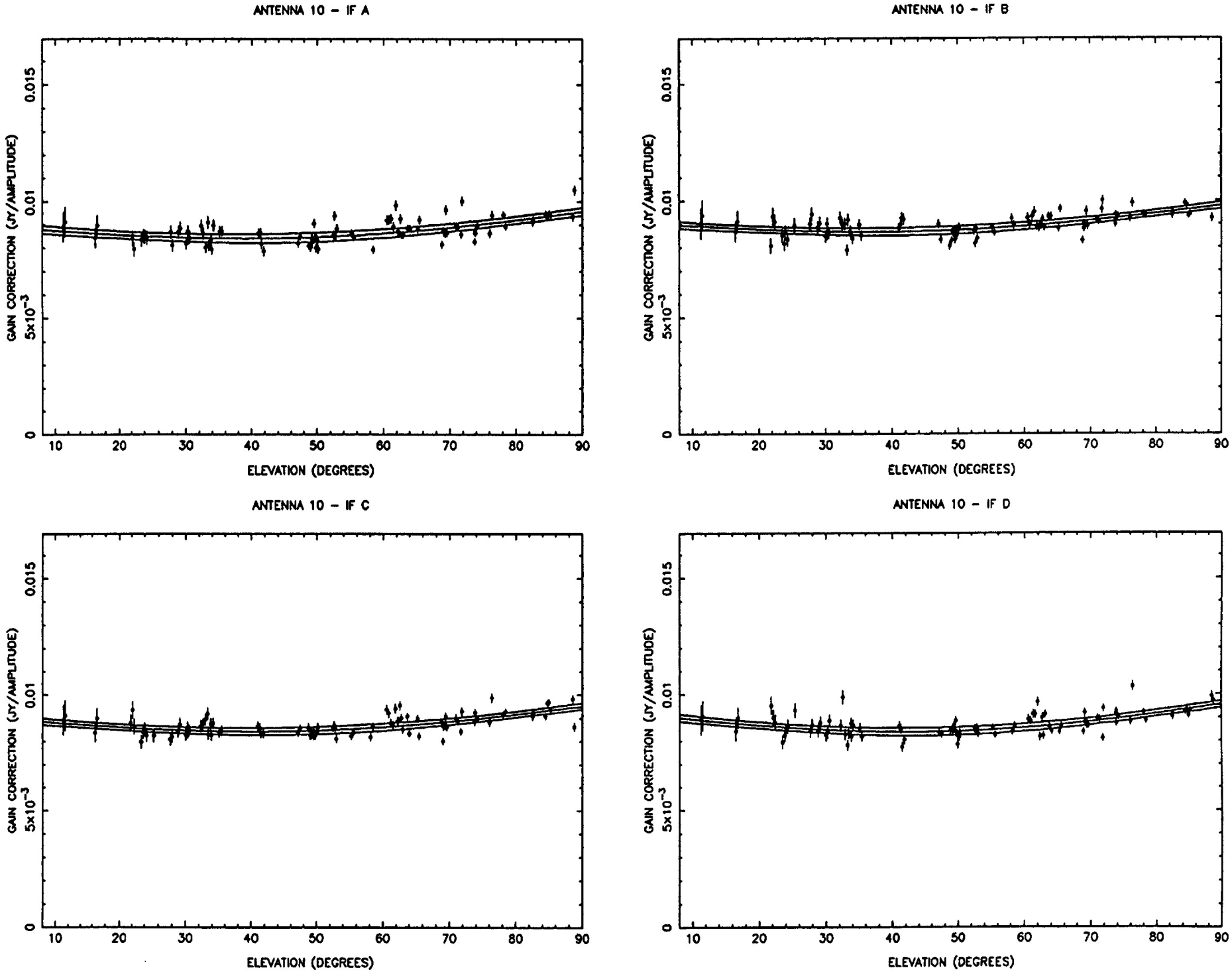
ANTENNA 10 - IF A
ANTENNA 10 - IF B
ANTENNA 10 - IF C
ANTENNA 10 - IF D
GAIN CORRECTION (JY/AMPLITUDE)
0
5x10^-3
0.01
0.015
10
20
30
40
50
60
70
80
90
ELEVATION (DEGREES)

FIGURE 10

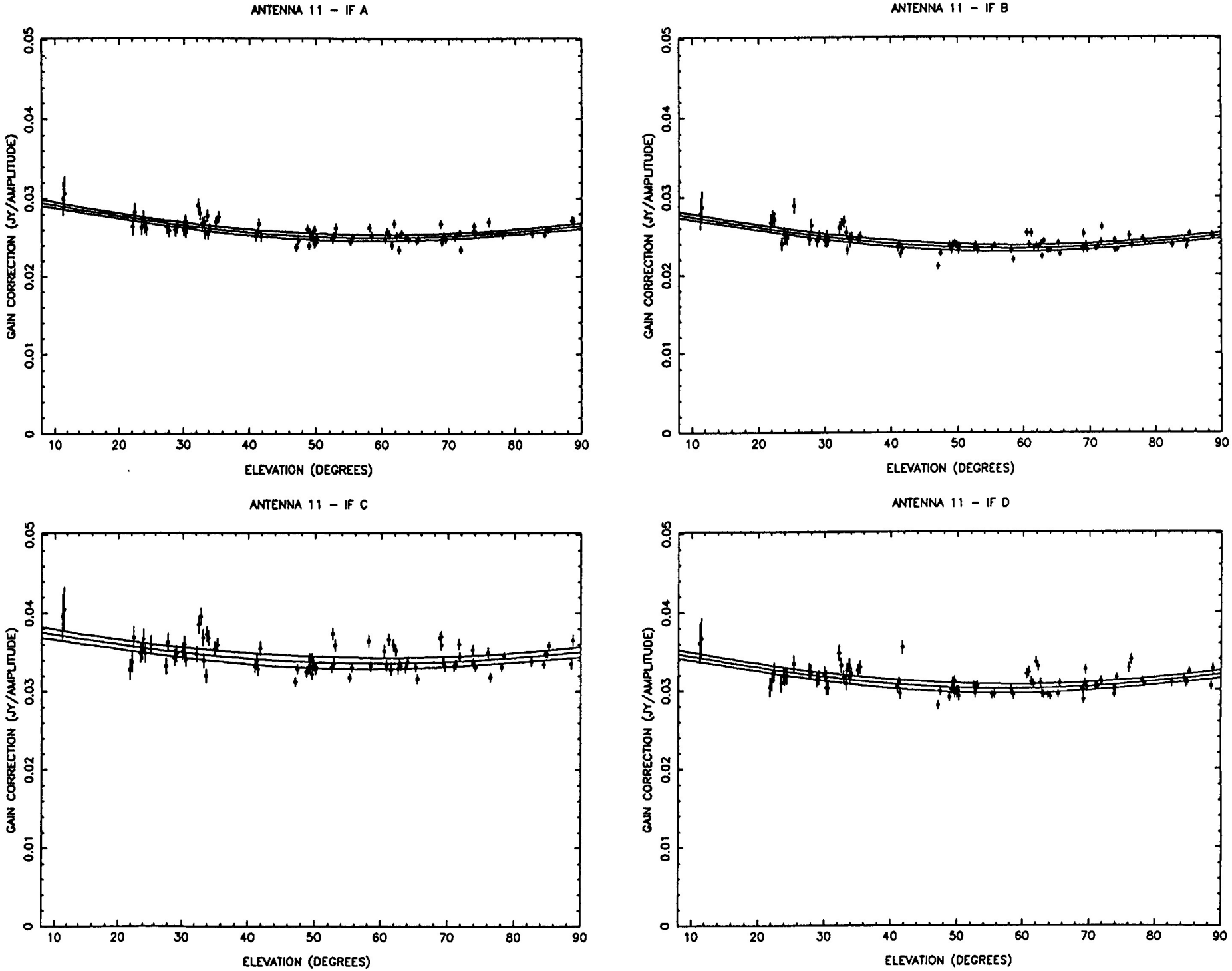
ANTENNA 11 - IF A
ANTENNA 11 - IF B
ANTENNA 11 - IF C
ANTENNA 11 - IF D
GAIN CORRECTION (JY/AMPLITUDE)
ELEVATION (DEGREES)
0
0.01
0.02
0.03
0.04
0.05
10
20
30
40
50
60
70
80
90

FIGURE 11

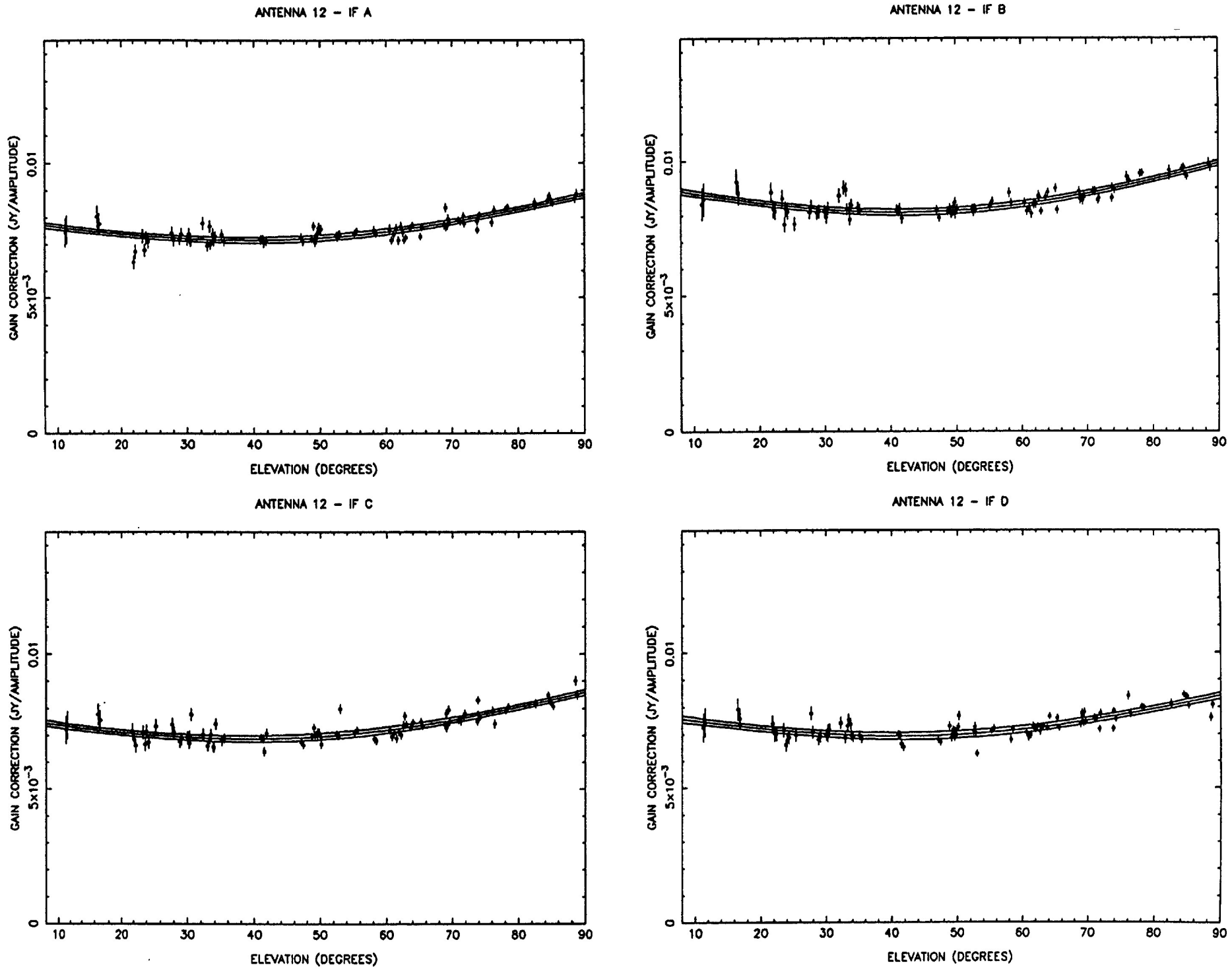
ANTENNA 12 - IF A
ANTENNA 12 - IF B
ANTENNA 12 - IF C
ANTENNA 12 - IF D
GAIN CORRECTION (JY/AMPLITUDE)
0
5x10^-3
0.01
10
20
30
40
50
60
70
80
90
ELEVATION (DEGREES)

FIGURE 12

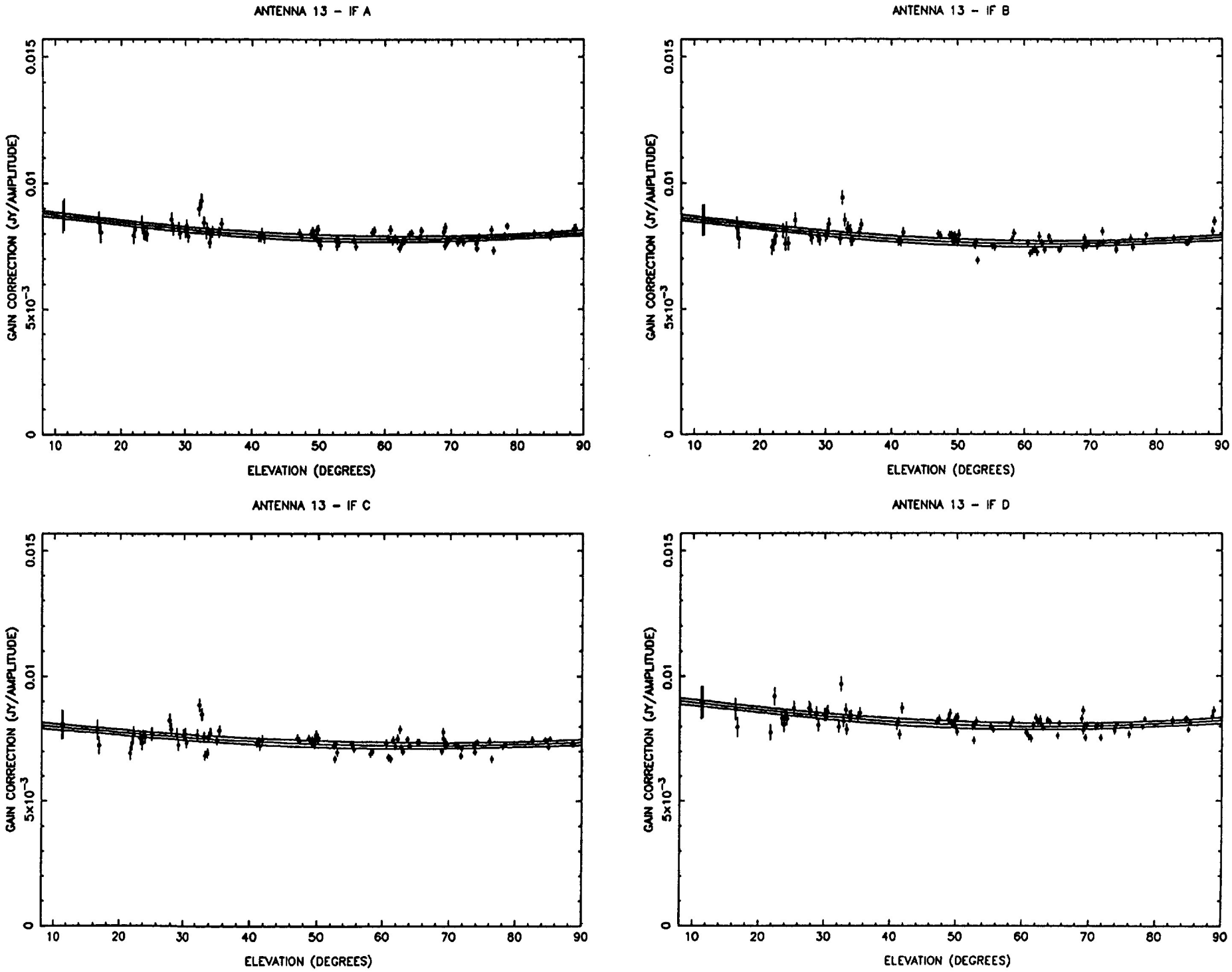
ANTENNA 13 - IF A
ANTENNA 13 - IF B
ANTENNA 13 - IF C
ANTENNA 13 - IF D
GAIN CORRECTION (JY/AMPLITUDE)
0
5x10⁻³
0.01
0.015
10
20
30
40
50
60
70
80
90
ELEVATION (DEGREES)

FIGURE 13

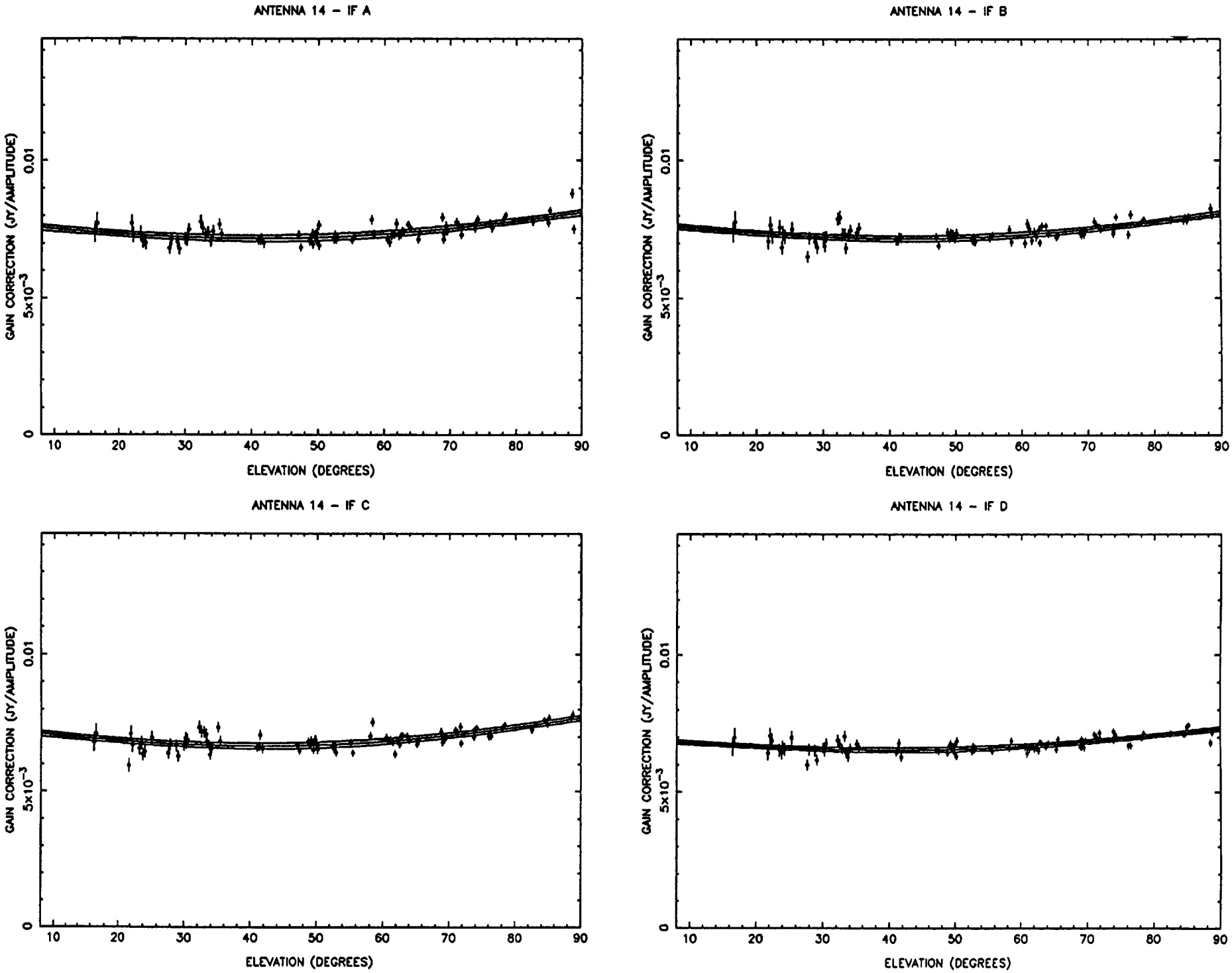
ANTENNA 14 - IF A
ANTENNA 14 - IF B
ANTENNA 14 - IF C
ANTENNA 14 - IF D
GAIN CORRECTION (JY/AMPLITUDE)
0
5x10^-3
0.01
10
20
30
40
50
60
70
80
90
ELEVATION (DEGREES)

FIGURE 14

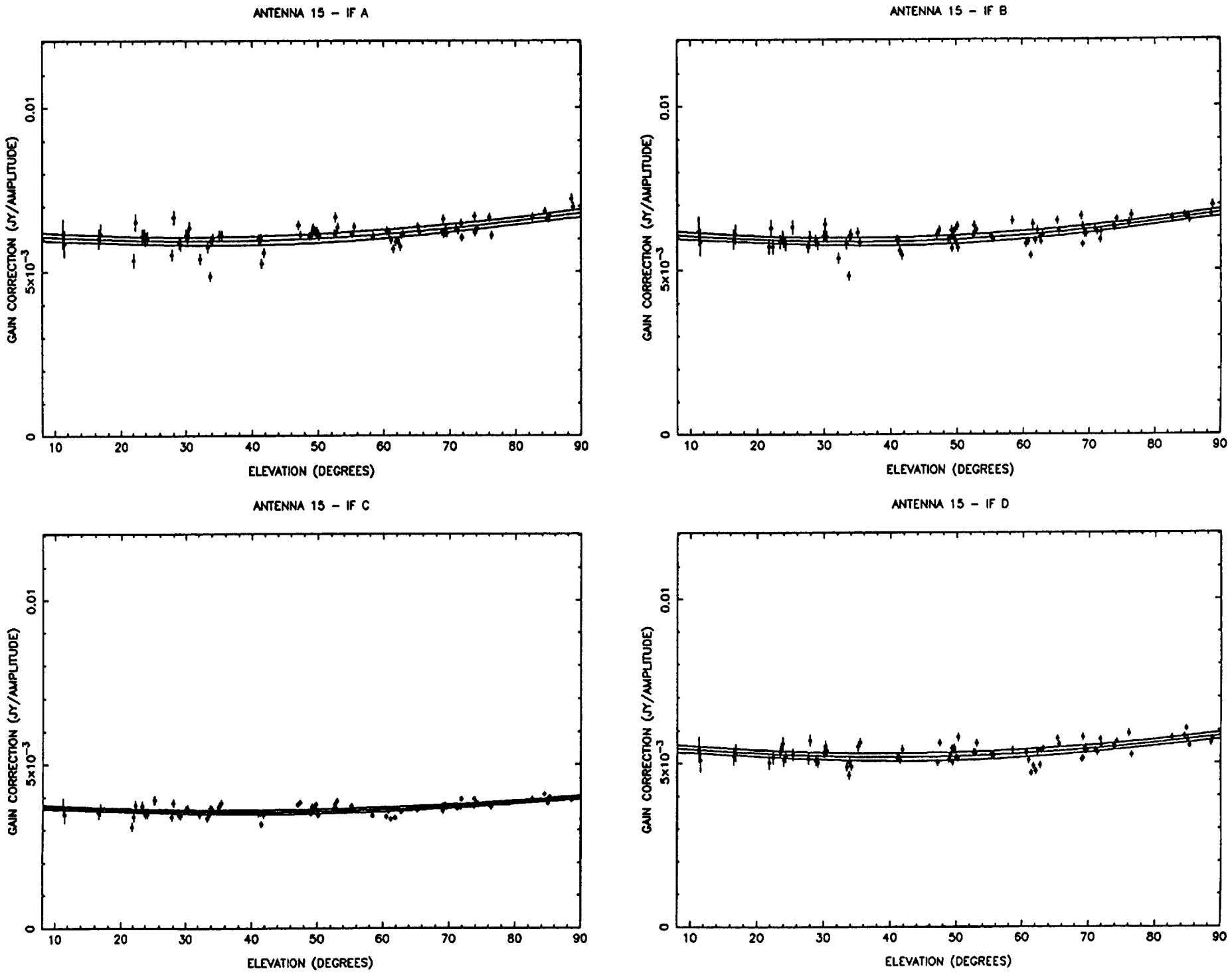
ANTENNA 15 - IF A
ANTENNA 15 - IF B
ANTENNA 15 - IF C
ANTENNA 15 - IF D
GAIN CORRECTION (JY/AMPLITUDE)
0
5x10^-3
0.01
10
20
30
40
50
60
70
80
90
ELEVATION (DEGREES)

FIGURE 15

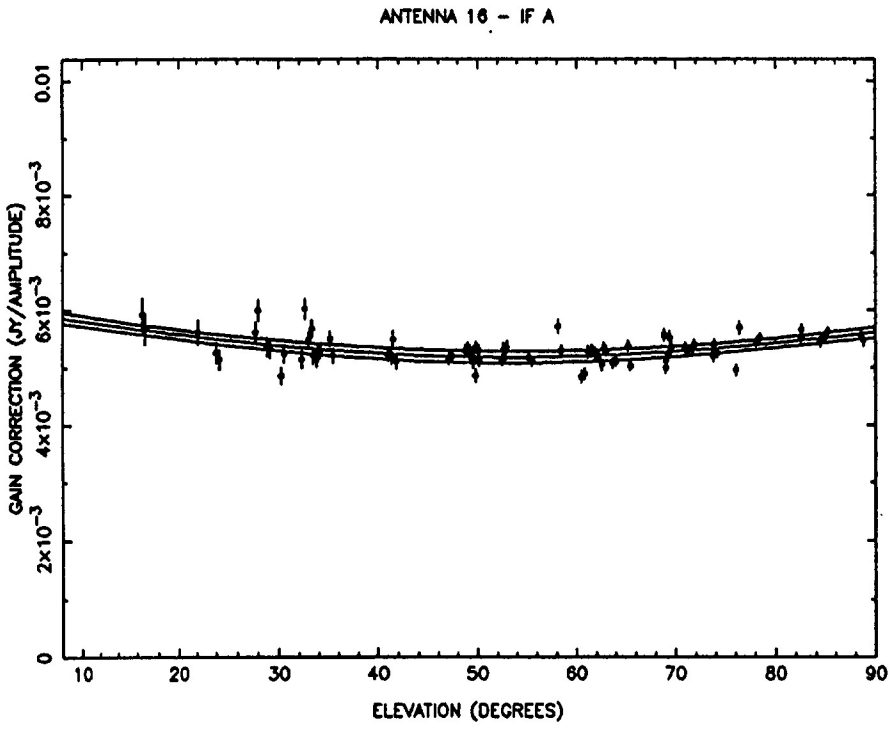
ANTENNA 16 - IF A
GAIN CORRECTION (JY/AMPLITUDE)
0
2x10⁻³
4x10⁻³
6x10⁻³
8x10⁻³
0.01
10
20
30
40
50
60
70
80
90
ELEVATION (DEGREES)

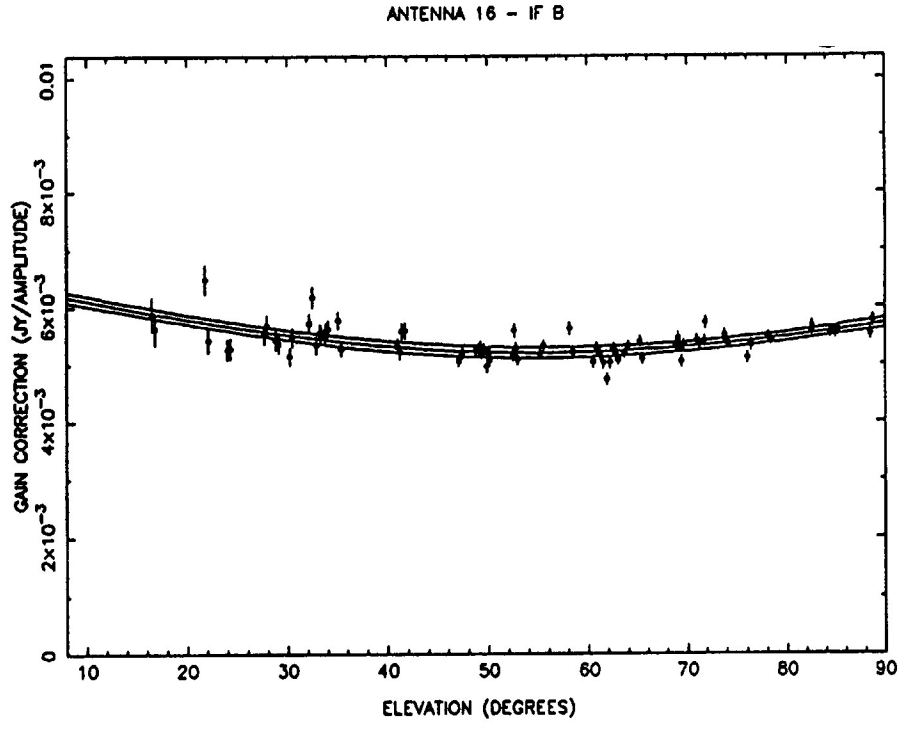
ANTENNA 16 - IF B
GAIN CORRECTION (JY/AMPLITUDE)
0
2x10⁻³
4x10⁻³
6x10⁻³
8x10⁻³
0.01
10
20
30
40
50
60
70
80
90
ELEVATION (DEGREES)

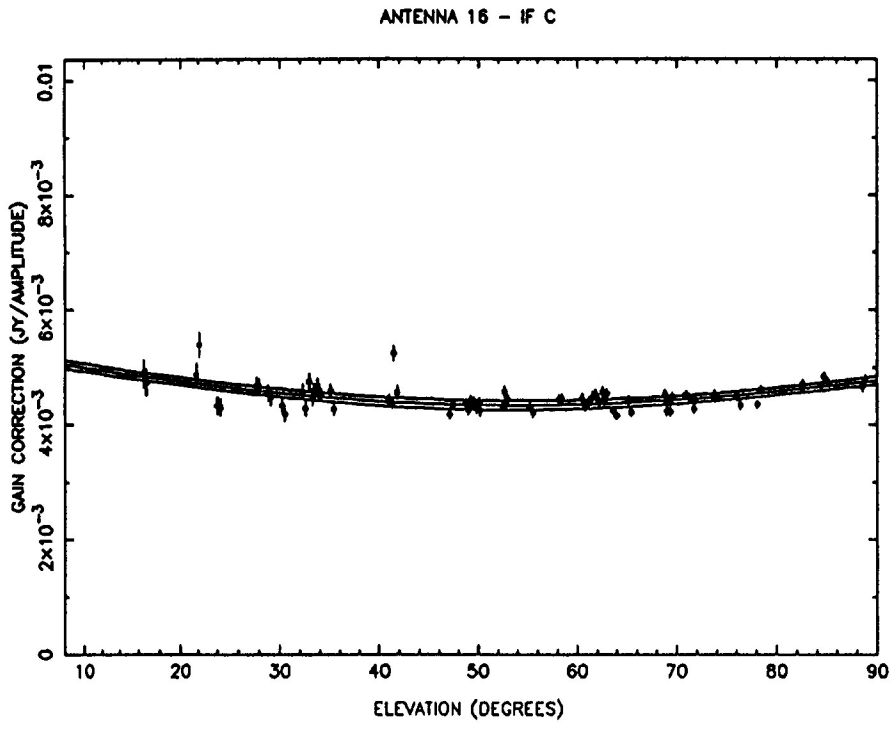
ANTENNA 16 - IF C
GAIN CORRECTION (JY/AMPLITUDE)
0
2x10⁻³
4x10⁻³
6x10⁻³
8x10⁻³
0.01
10
20
30
40
50
60
70
80
90
ELEVATION (DEGREES)

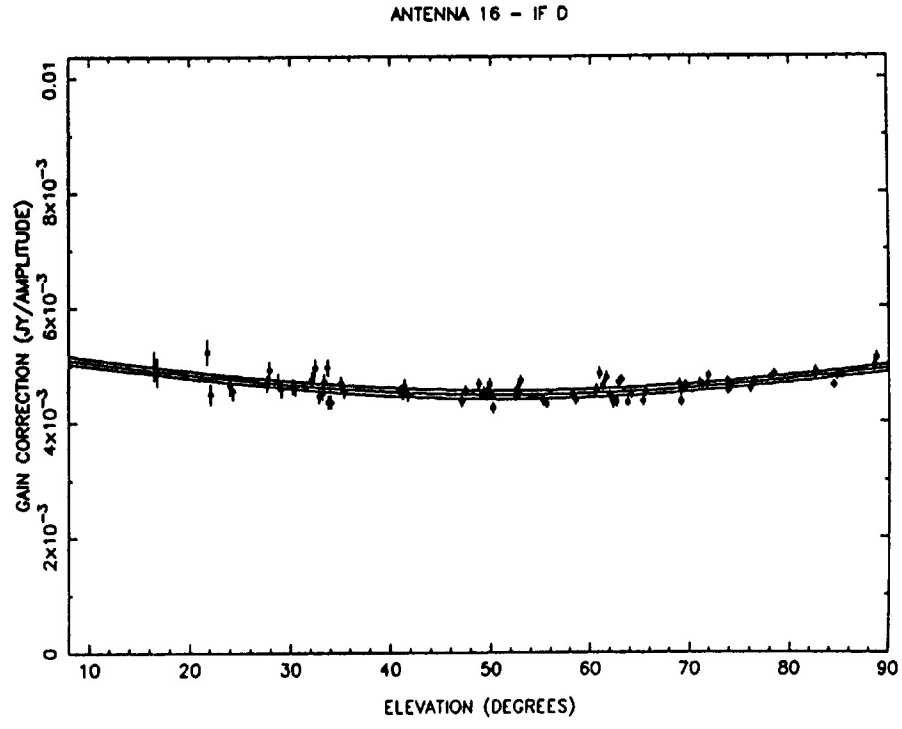
ANTENNA 16 - IF D
GAIN CORRECTION (JY/AMPLITUDE)
0
2x10⁻³
4x10⁻³
6x10⁻³
8x10⁻³
0.01
10
20
30
40
50
60
70
80
90
ELEVATION (DEGREES)

FIGURE 16

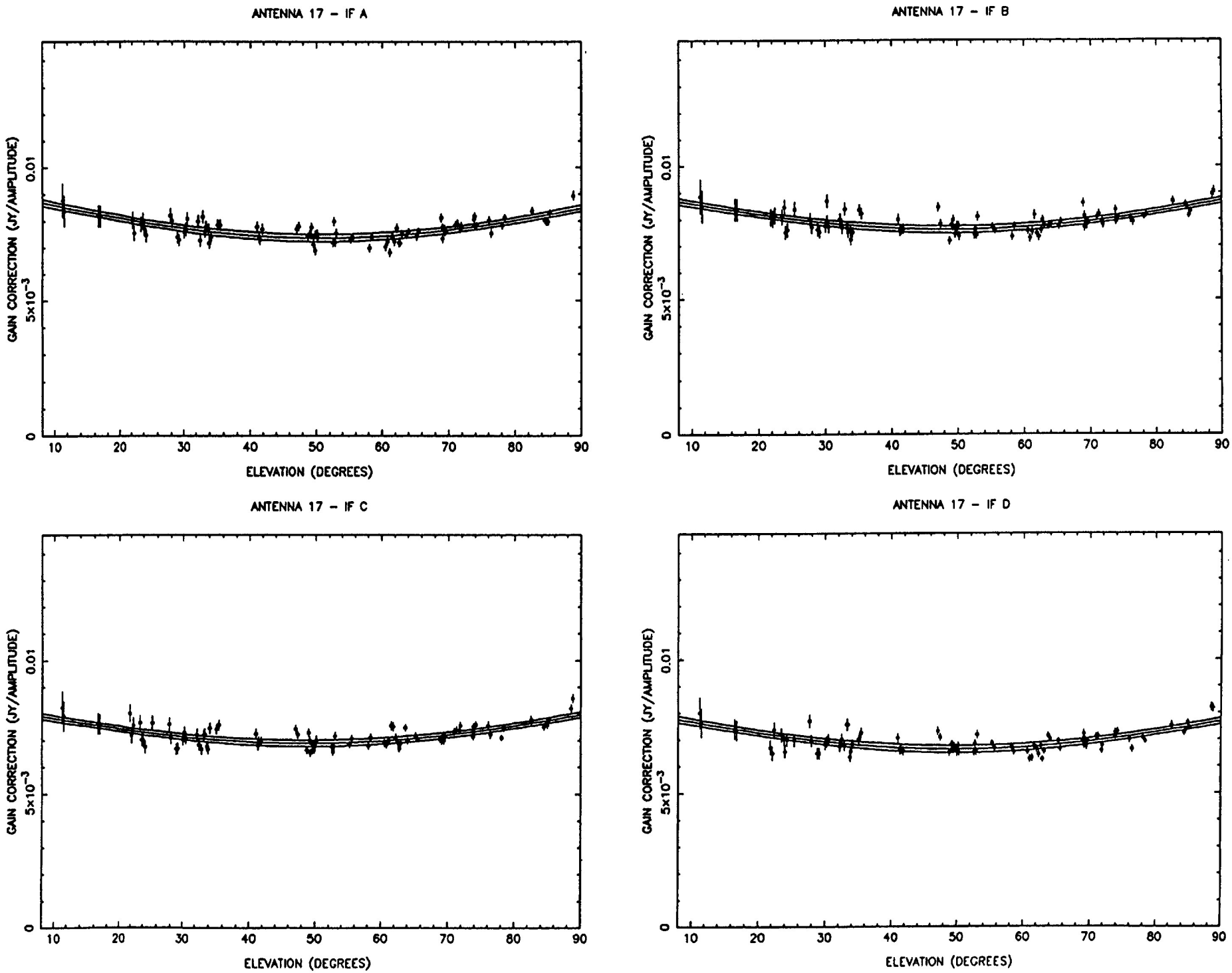
ANTENNA 17 - IF A
ANTENNA 17 - IF B
ANTENNA 17 - IF C
ANTENNA 17 - IF D
GAIN CORRECTION (JY/AMPLITUDE)
0
5x10^-3
0.01
10
20
30
40
50
60
70
80
90
ELEVATION (DEGREES)

FIGURE 17

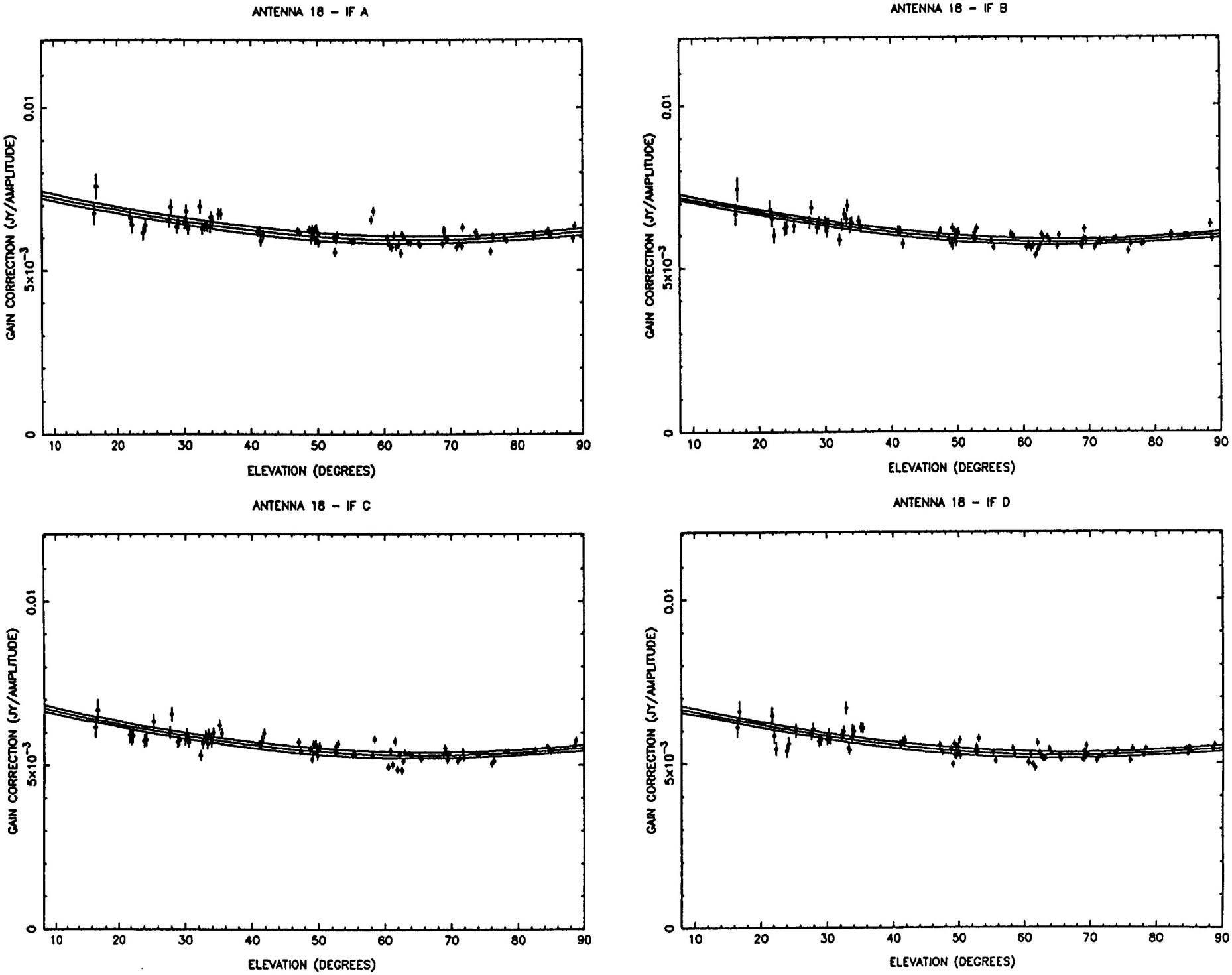
ANTENNA 18 - IF A
ANTENNA 18 - IF B
ANTENNA 18 - IF C
ANTENNA 18 - IF D
GAIN CORRECTION (JY/AMPLITUDE)
0
5x10^-3
0.01
10
20
30
40
50
60
70
80
90
ELEVATION (DEGREES)

FIGURE 18

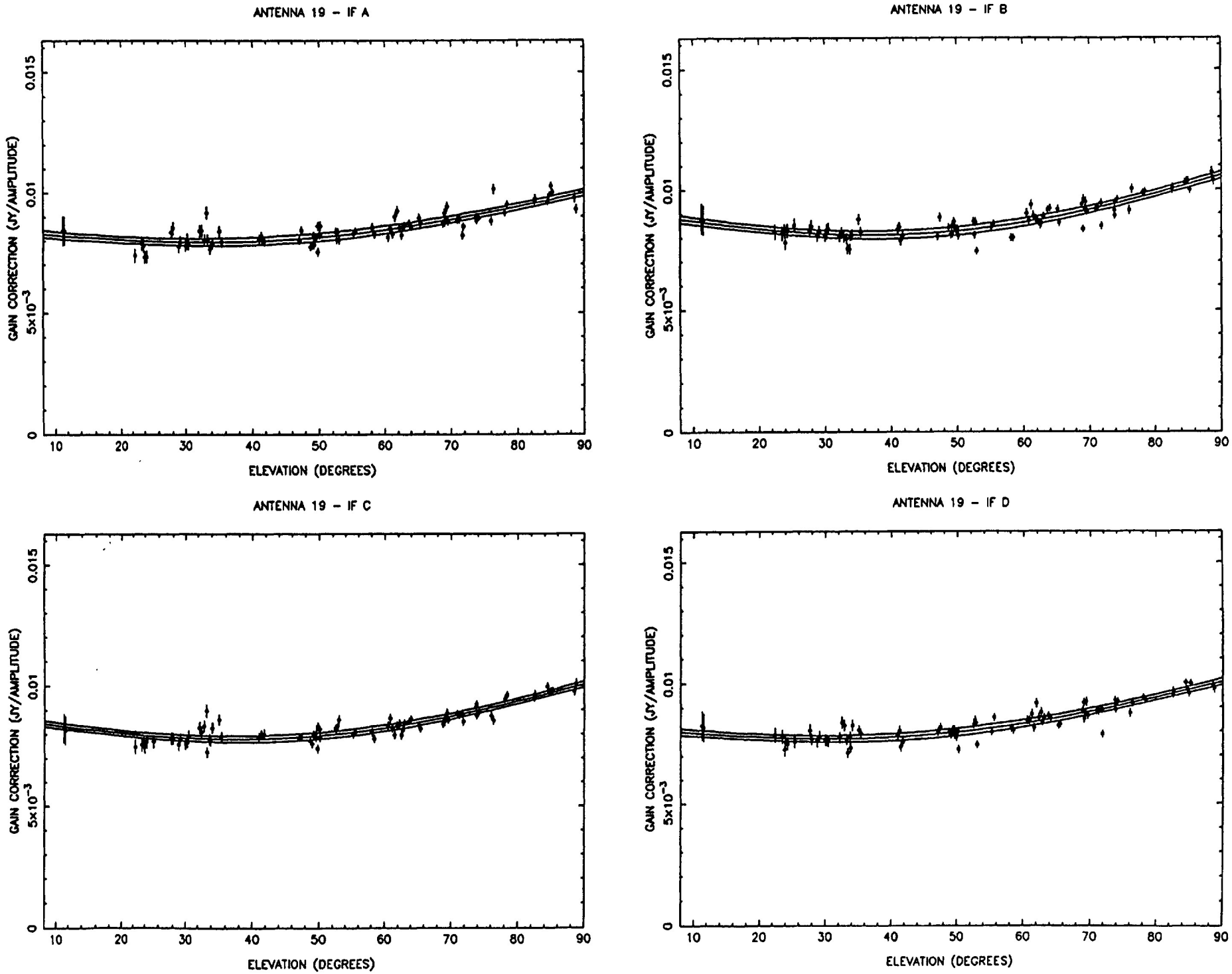
ANTENNA 19 - IF A
ANTENNA 19 - IF B
ANTENNA 19 - IF C
ANTENNA 19 - IF D
GAIN CORRECTION (JY/AMPLITUDE)
0
5x10⁻³
0.01
0.015
10
20
30
40
50
60
70
80
90
ELEVATION (DEGREES)

FIGURE 19

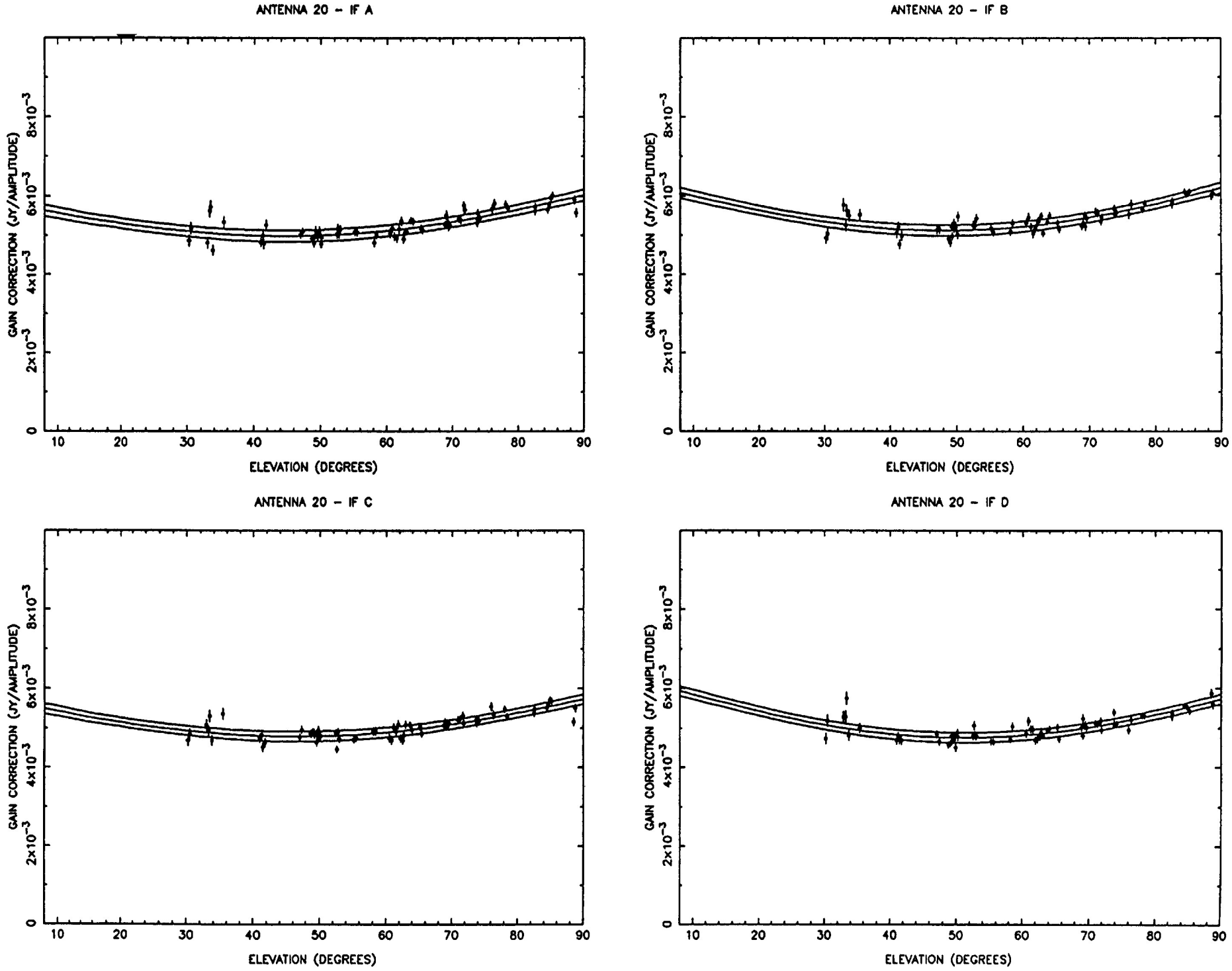
ANTENNA 20 - IF A
ANTENNA 20 - IF B
ANTENNA 20 - IF C
ANTENNA 20 - IF D
GAIN CORRECTION (JY/AMPLITUDE)
0
2x10^-3
4x10^-3
6x10^-3
8x10^-3
10
20
30
40
50
60
70
80
90
ELEVATION (DEGREES)

FIGURE 20

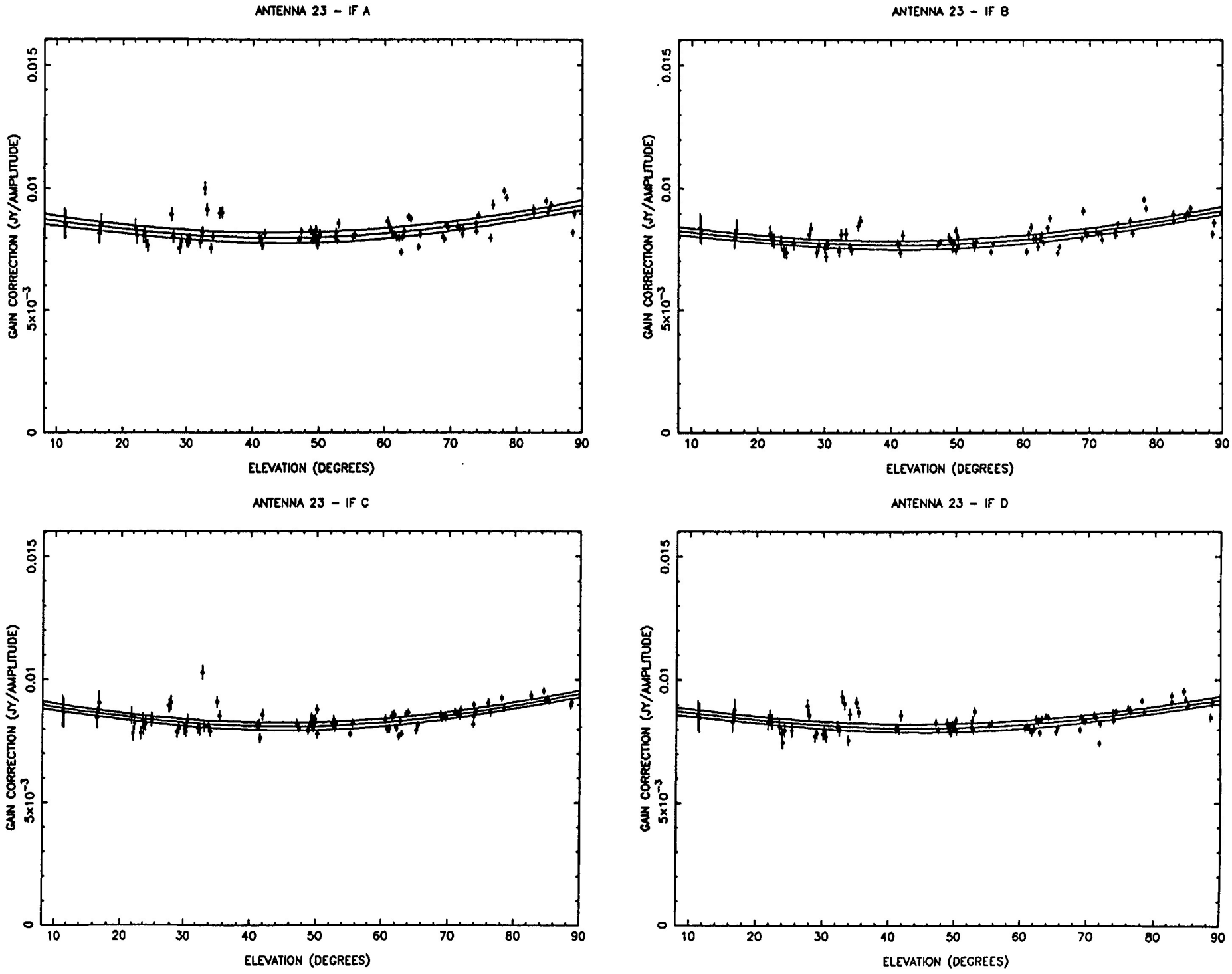
ANTENNA 23 - IF A
ANTENNA 23 - IF B
ANTENNA 23 - IF C
ANTENNA 23 - IF D
GAIN CORRECTION (JY/AMPLITUDE)
0
5x10^-3
0.01
0.015
10
20
30
40
50
60
70
80
90
ELEVATION (DEGREES)

FIGURE 21

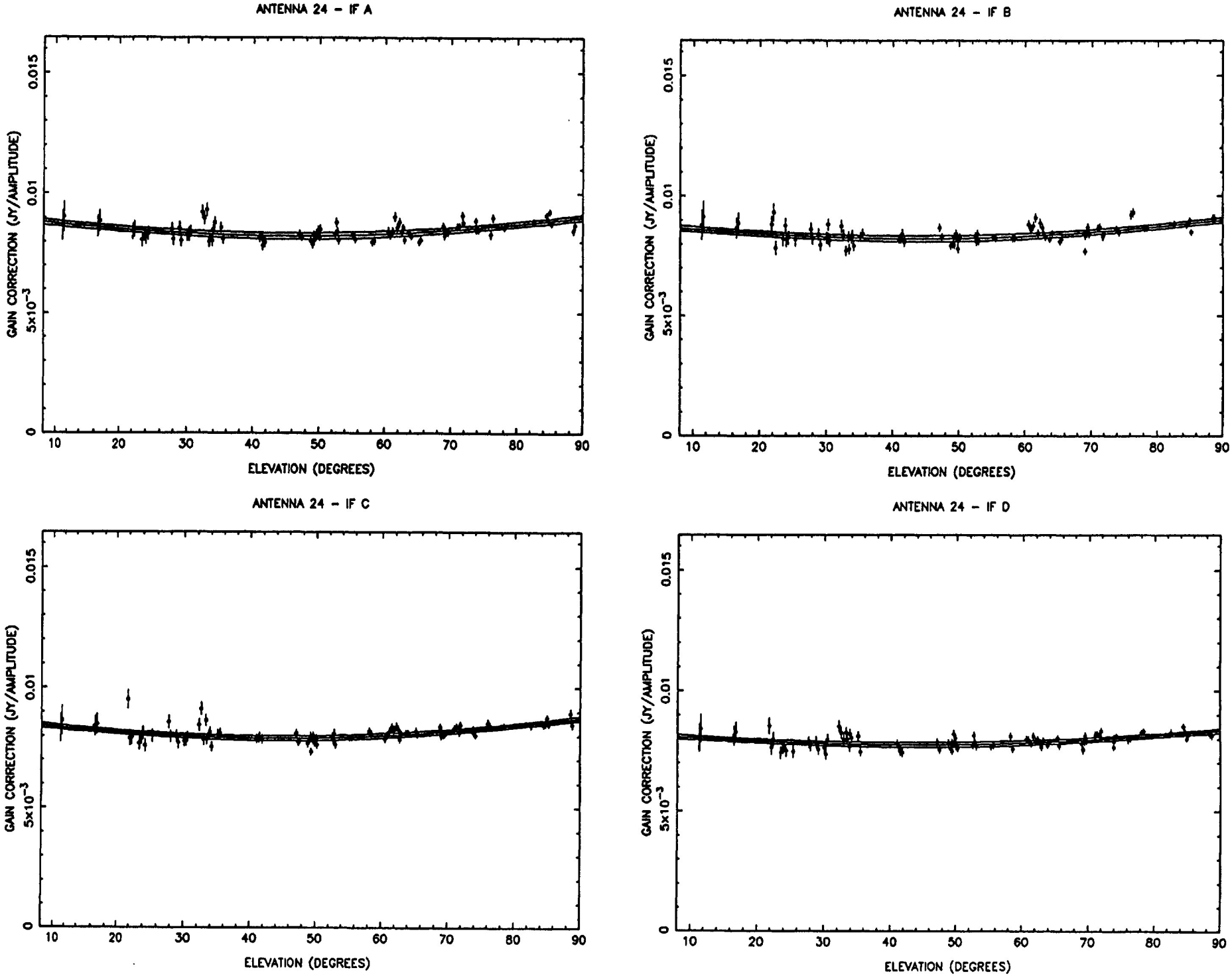
ANTENNA 24 - IF A
ANTENNA 24 - IF B
ANTENNA 24 - IF C
ANTENNA 24 - IF D
GAIN CORRECTION (JY/AMPLITUDE)
0
5x10^-3
0.01
0.015
10
20
30
40
50
60
70
80
90
ELEVATION (DEGREES)

FIGURE 22

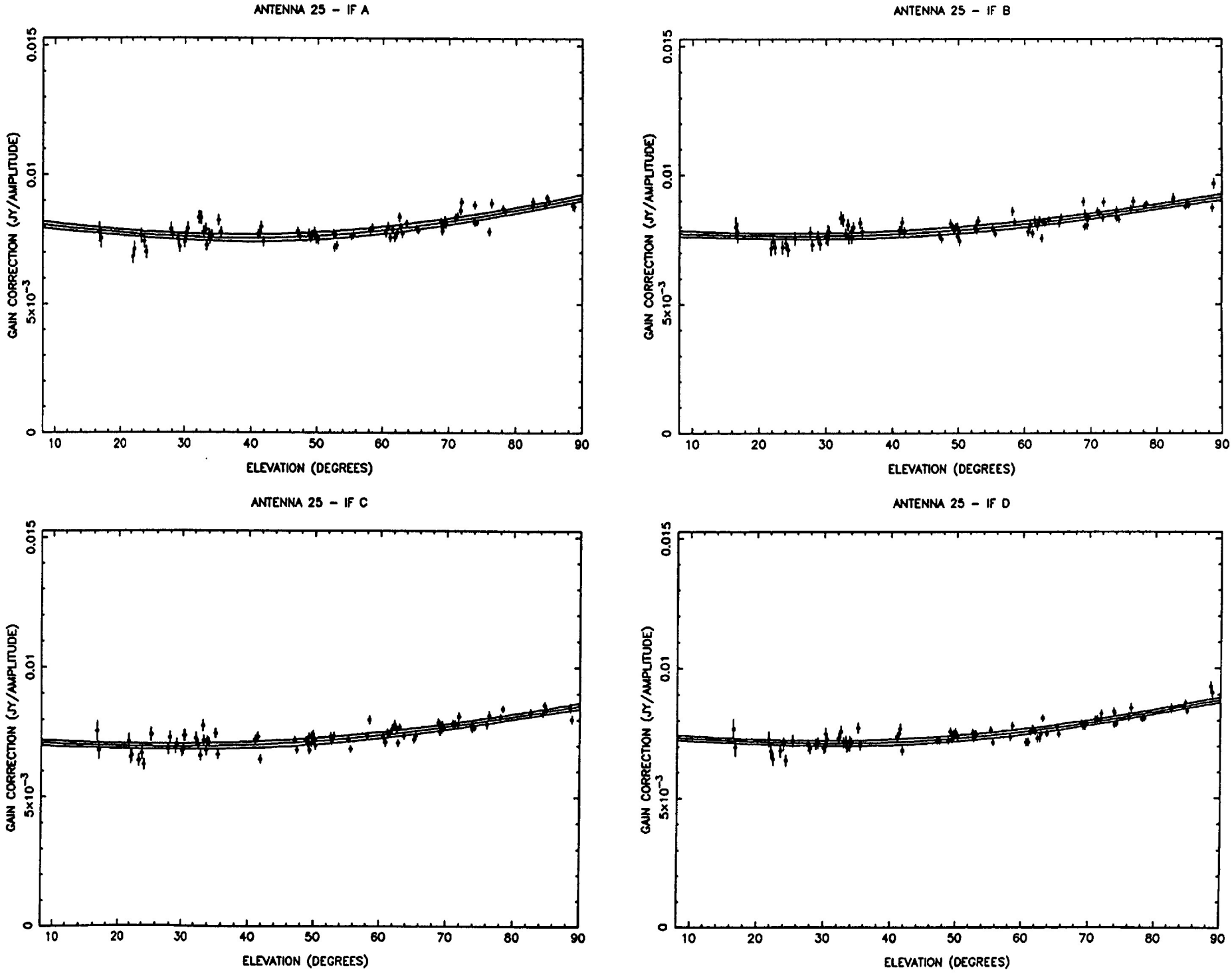
ANTENNA 25 - IF A
ANTENNA 25 - IF B
ANTENNA 25 - IF C
ANTENNA 25 - IF D
GAIN CORRECTION (JY/AMPLITUDE)
0
5x10⁻³
0.01
0.015
10
20
30
40
50
60
70
80
90
ELEVATION (DEGREES)

FIGURE 23

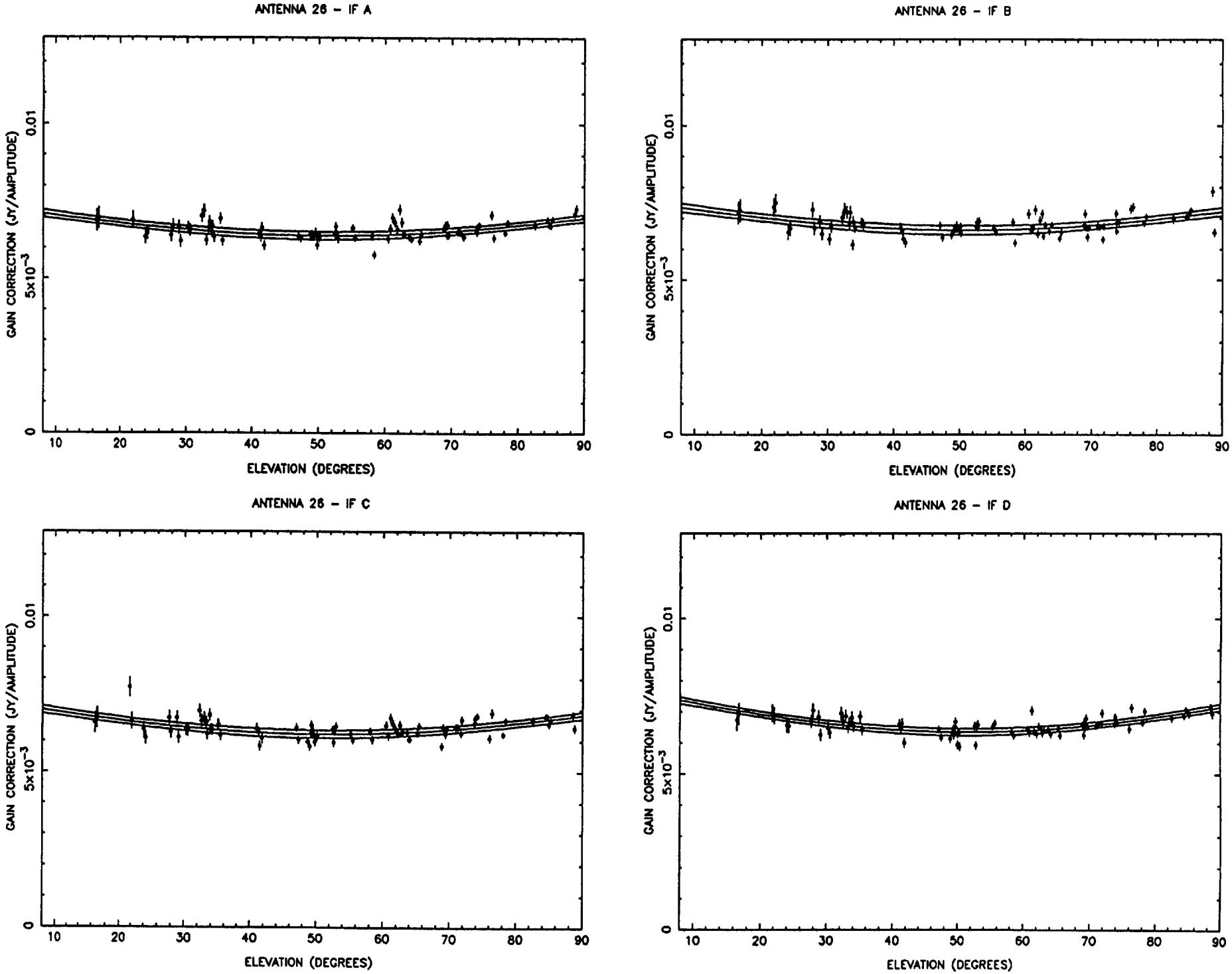
ANTENNA 26 - IF A
ANTENNA 26 - IF B
ANTENNA 26 - IF C
ANTENNA 26 - IF D
GAIN CORRECTION (JY/AMPLITUDE)
0
5x10^-3
0.01
10
20
30
40
50
60
70
80
90
ELEVATION (DEGREES)

FIGURE 24

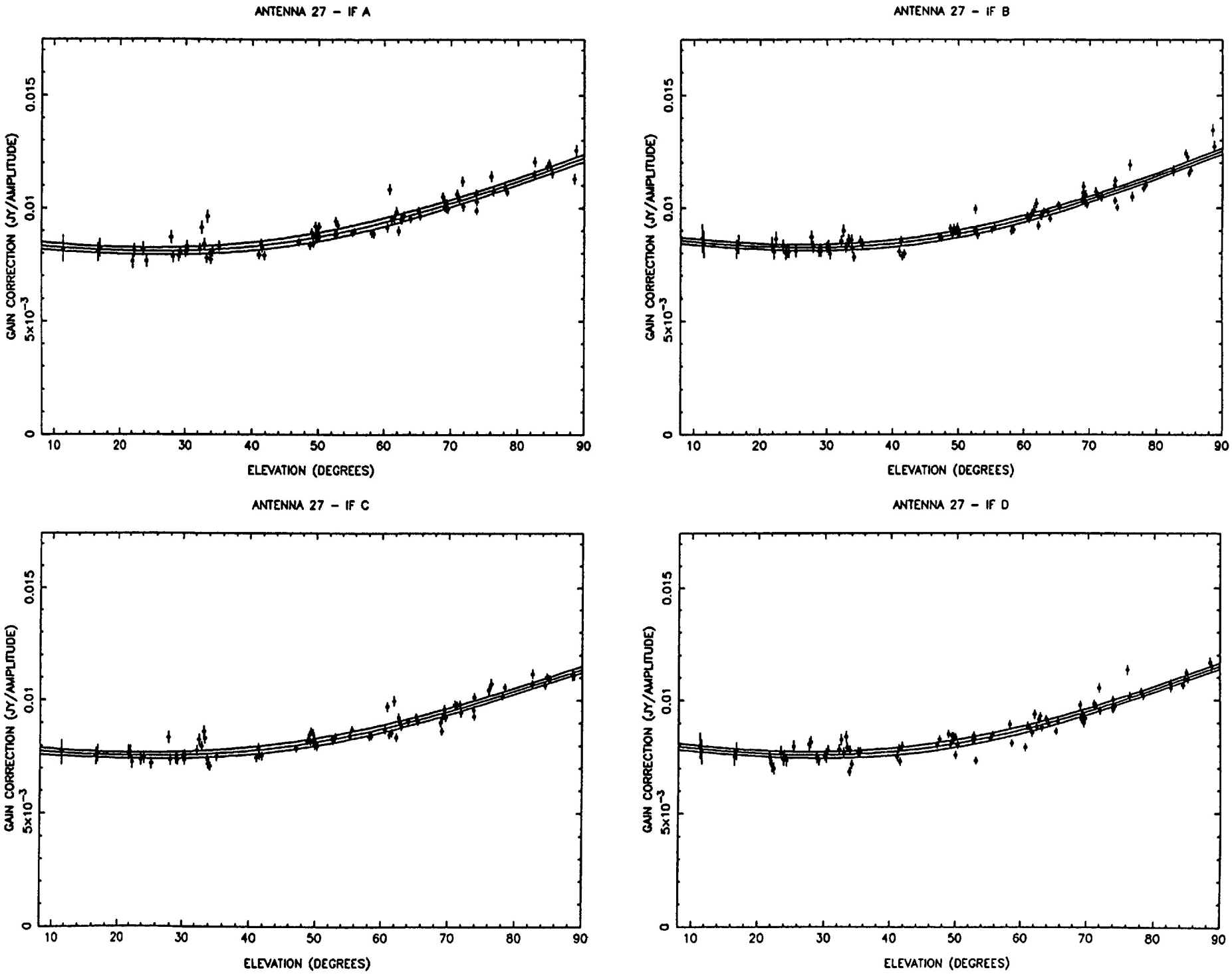
ANTENNA 27 - IF A
ANTENNA 27 - IF B
ANTENNA 27 - IF C
ANTENNA 27 - IF D
GAIN CORRECTION (JY/AMPLITUDE)
0
5x10^-3
0.01
0.015
10
20
30
40
50
60
70
80
90
ELEVATION (DEGREES)

FIGURE 25

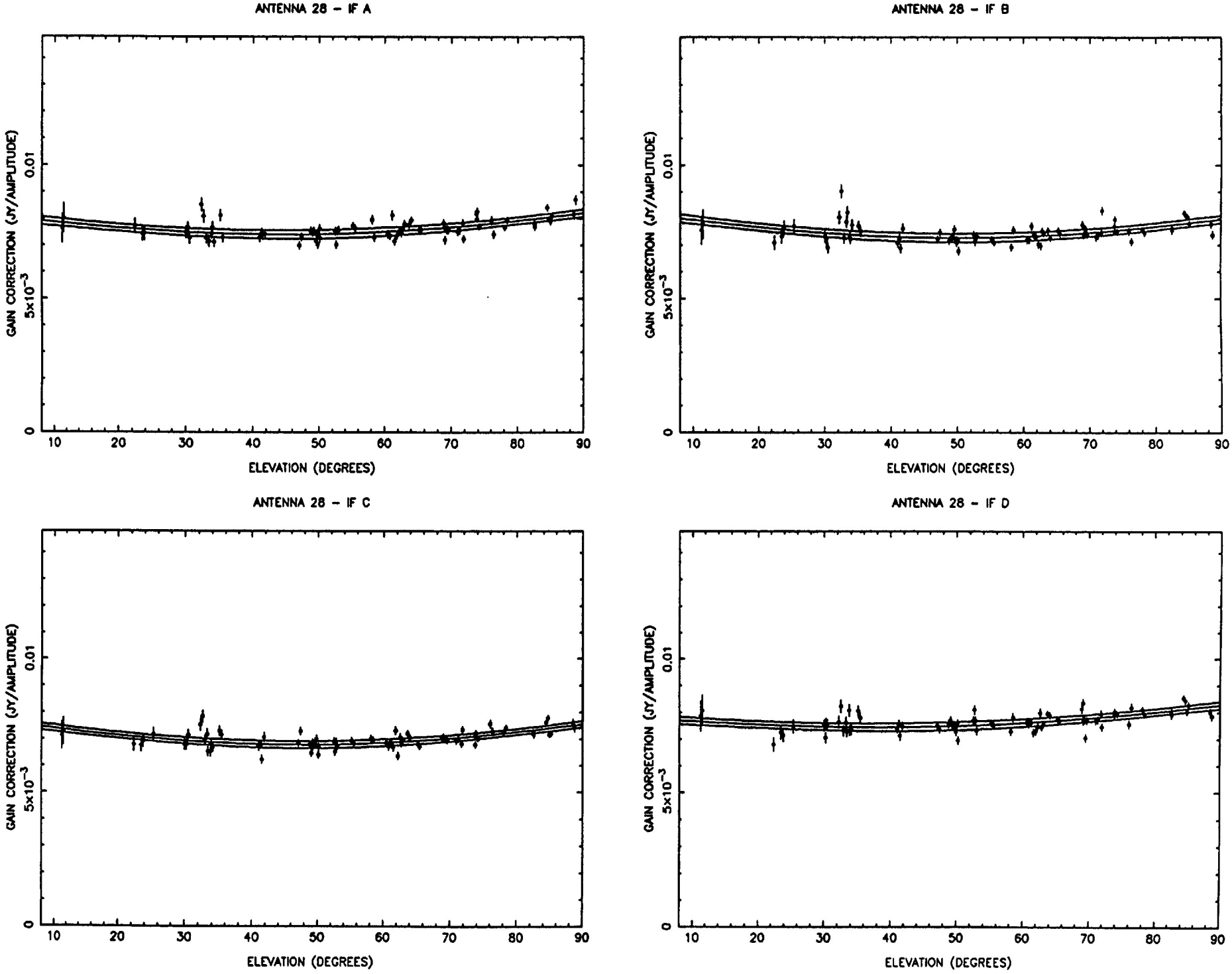
ANTENNA 28 - IF A
ANTENNA 28 - IF B
ANTENNA 28 - IF C
ANTENNA 28 - IF D
GAIN CORRECTION (JY/AMPLITUDE)
0
5x10⁻³
0.01
10
20
30
40
50
60
70
80
90
ELEVATION (DEGREES)

FIGURE 26

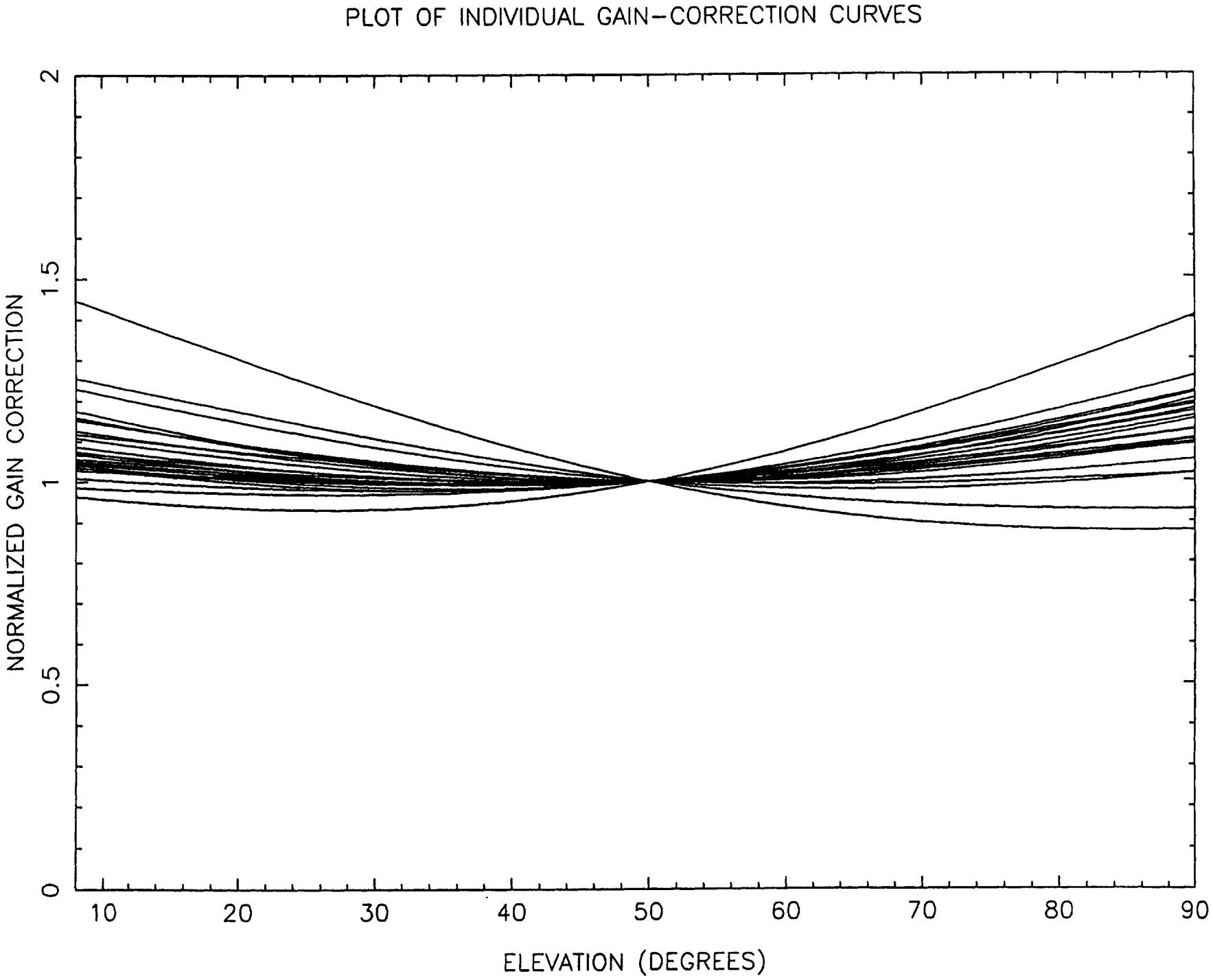
PLOT OF INDIVIDUAL GAIN-CORRECTION CURVES
NORMALIZED GAIN CORRECTION
0
0.5
1
1.5
2
10
20
30
40
50
60
70
80
90
ELEVATION (DEGREES)

FIGURE 27